Solid/liquid ratios of trace elements and radionuclides during a Nuclear Power Plant liquid discharge in the Seine River: Field measurements vs geochemical modeling

Svetlana Ilina, Laura Marang, Beatriz Louriño-Cabana, Frederique Eyrolle, Patrick Boyer, Frederic Coppin, Yann Sivry, Alexandre Gélabert, Marc F. Benedetti

HAL Id: hal-02648303
https://hal.science/hal-02648303

Submitted on 29 May 2020

Solid/liquid ratios of trace elements and radionuclides during a Nuclear Power Plant liquid discharge in the Seine River: Field measurements vs geochemical modelling

Svetlana M. Ilina[1], Laura Marang[2], Beatriz Lourino-Cabana[2], Frédérique Eyrolle[3], Patrick Boyer[3], Frederic Coppin[3], Yann Sivry[1], Alexandre Gélabert[1], Marc F. Benedetti[1*]

[1]Université de Paris, Institut de physique du globe de Paris, CNRS, F-75005 Paris, France
[2] EDF R&D LNHE - Laboratoire National d'Hydraulique et Environnement, 6 quai Watier, 78401 Chatou, France
[3] Institut de Radioprotection et de Sûreté Nucléaire (IRSN) PSE-ENV/SRTE/, SRTE/, Cadarache, Saint Paul Lez Durance, 11315, France

- Corresponding author
- Professor : Marc F. Benedetti
- Université de Paris, Institut de physique du globe de Paris, CNRS, IGN,
- 1 rue Jussieu F-75238 Paris, France
- E-mail address: benedetti@ipgp.fr

Abstract

This study focuses on the determination of field solid/liquid ratios (Rd) values of trace element (TE) and radionuclide (RN) in the Seine River (France) during a concerted low radioactivity level liquid regulatory discharge performed by a Nuclear Power Plant (NPP) and their confrontation with Kd values calculated from geochemical modeling. This research focuses on how field Rd measurements of TE and RN can be representative of Kd values and how Kd models should be improved.

For this purpose 5 sampling points of the Seine River during a NPP's liquid discharge were investigated: upstream from the discharge in order to assess the natural background values in the area of effluent discharge, the total river water mixing distance (with transect sampling), and 2 points downstream from this last area. The main parameters required determining field Rd of TE and RN and their geochemical modeling (Kd) were acquired. Filtered waters were analyzed for alkalinity, anions, cations, dissolved organic carbon (DOC), TE, and RN concentrations. Suspended particulate matter (SPM) was analyzed for particulate organic carbon (POC), TE and RN concentrations and mineralogical composition. Field Rd and Kd values are in good agreement for stable Cd, Cu, Ni, Pb and Zn and for ^{7}Be. Conversely, measured field Rd for stable Ag, Ba, Sr, Co and Cs are systematically higher than modeled Kd values. Even if only the lowest possible values were obtained for ^{137}Cs and ^{60}Co Rd measurements, these estimated limits are higher than calculated Kd for ^{137}Cs and in good agreement for ^{60}Co. Finally, only two RN exhibit field Rd lower than calculated Kd: ^{234}Th and ^{210}Pb.

Comparison of field Rd vs. modeled Kd values for TE and RN allows the identification, for each element, of the main involved adsorption phases and geochemical mechanisms controlling their fate and partitioning in river systems.

Keywords: radionuclides, trace elements, partition coefficient, geochemical modeling, River

Highlights:

- This research focuses on how field solid/liquid ratios (Rd) measurements of trace elements and radionuclides can be representative of Kd values and how Kd models should be improved.

- Field Rd measurements and modeled Kd values are in good agreement for stable Cd, Cu, Ni, Pb and Zn and for ^{7}Be

- Comparison of field Rd vs. modelled Kd values for trace elements and radionuclides allows the identification of the main geochemical mechanisms controlling their fate and partitioning in river systems.

1 Introduction

The distribution (or partitioning) coefficient (Kd) between soluble and particulate phases is one of the most important parameters used in estimating the mobility of trace elements or radionuclides (TE or RN) in fresh, estuarine and marine waters. Partition coefficients help to assess health and environmental risks because they allow quantifying pathways of environmental transport, spatial and temporal distributions, mobility and bioavailability of trace element and radionuclides (Sibley *et al.*, 1986; Benes *et al.*, 1992, 1994; Ciffroy *et al.*, 2001; Brach-Papa *et al.*, 2005). Trace element and radionuclide, characterized by high Kd values exhibit low mobility within water bodies and predominant transfer pathways through physical dispersion of solid particles. Those characterized by low Kd values are mainly exported within water fluxes and their concentrations in the environment fluctuate more rapidly than those of the former group (Vesely *et al.*, 2001). Kd is defined as the ratio of the trace element and radionuclides concentration sorbed onto naturally occurring solid surfaces to their corresponding concentration in the dissolved phase of the surrounding water mass. Using Kd parameter assumes that (1) only low concentration of trace element and radionuclide are both in aqueous and solid phases, (2) relationship between their concentrations in the solid and liquid phases is linear, (3) equilibrium conditions are reached, (4) similar and reversible rapid adsorption and desorption kinetics are observed, (5) it describes trace element and radionuclide partitioning between one single sorbate (TE and RN) and one unique sorbent type (soil, particular matter, sediments, etc.), and (6) all adsorption sites are accessible and have equal strength (EPA, 1999). Most Kd values used in environmental and health risks assessment originate from the literature after statistical analyses (J. Allison and T. Allison, 2005; IAEA, 2010). Kd values are usually derived from field solid/liquid ratios (Rd) obtained from laboratory or field experiments and depend on the nature of adsorbent and on the chemical conditions of the aqueous media used. However,

26 laboratory experiments determine Rd values for a predominant process or a single sorbent

27 associated with a given chemical solution composition (Radovanovic and Koelmans, 1998;

28 Tipping *et al.*, 1998; Vesely *et al.*, 2001). Thereby, Kd values are not necessarily suitable

29 and/or available for a wide range of river systems. Most generally, they represent an

30 integrative representation of complex processes controlling solid/liquid partitioning including

31 various parameters such as suspended particulate matter (SPM) concentration, composition

32 and origin (Zhao and Hou, 2012), major and trace element concentrations (Lourino-Cabana *et*

33 *al.*, 2010), pH value (EPA, 1999), water temperature, redox conditions (Bird and Schwartz,

34 1997; Xue *et al.*, 1997), ionic strength, organic matter (OM) concentration and nature (Bryan

35 *et al.*, 2002; Pokrovsky *et al.*, 2010) and climatic settings (O'Connor and Connolly, 1980;

36 Garnier *et al.*, 1997; J. Allison and T. Allison, 2005). Thus, the relevance and robustness of

37 literature-derived Kd values most generally highly depend on both the number of referenced

38 data and physico-chemical information associated to those data. As Kd values ranging over

39 until five orders of magnitude can be obtained from literature (EPA, 1999; IAEA, 2010;

40 Boyer *et al.*, 2017; Tomczak et al., 2019), using generic or default Kd values can result in

41 significant uncertainties when they are used to predict the fate of trace element and

42 radionuclide. Thereby, site-specific Kd values are required for site-specific trace element and

43 radionuclide and risk assessment calculations. Ideally, site-specific Kd values should be

44 deduced from field Rd measured for a huge range of biogeochemical conditions

45 characterizing the target ecosystem, which is generally not the most common case. It is

46 therefore crucial to link Kd values with realistic environmental physico-chemical settings

47 before they are applied to trace element and radionuclide transport modeling in rivers

48 submitted to discharges from Nuclear Power Plant (NPP's) (Ciffroy *et al.*, 2000, 2009).

49   In this frame, the main objectives of our study were (1) to acquire field Rds for trace

50 element and radionuclide during a NPP's liquid discharge from regulatory operations in the

51　Seine River; (2) to apply a geochemical speciation modeling for Kd calculation by using

52　physico-chemical parameter values measured at the various sampling points as input data; (3)

53　to compare calculated Kd values to the field Rds of trace element and radionuclide in order to

54　improve and to refine the geochemical models.

55

56　2. Materials and methods

57　　**2.1. Field settings, sampling sites, sampling procedure and sample treatment**

58　　　The study area is located within the Seine River upstream and downstream of La Motte-

59　Tilly (Fig. 1). The Seine River drains a typical Mesozoic-Cenozoic sedimentary basin

60　constituted of limestone mixed or inter bedded with terrigenous sediments derived from the

61　paleo reliefs bordering the Mesozoic and Cenozoic seas (Roy *et al.*, 1999). The Seine Basin is

62　characterized by a temperate and oceanic climate and is nearly uniform in terms of relief,

63　geology and hydrology. The hydrological regime is pluvial oceanic, with mean rainfall

64　between 500 and 1000 mm/year (Meybeck *et al.*, 2004). Detailed description of the Seine

65　River regarding the flow rates and their seasonal variations, geological settings and climatic

66　regime are described in details in Guérini *et al.*, 1998; Roy *et al.*, 1999; Ciffroy *et al.*, 2000;

67　Meybeck *et al.*, 2004; Billen *et al.*, 2007; Even *et al.*, 2007.

68　　　Fig. 1 and Fig. 2 present a simplified scheme of the Seine river watershed, along with

69　the sampling points, and the synthesis of analysis conducted and carrier phases taken into

70　account in the Kd calculation, respectively. Sample inventory and associated characteristics

71　are presented in Table 1. Samples were collected in august 2013 during a scheduled NPP's

72　liquid discharge at the most upstream station as a natural background values point (COP-1), at

73　the regulatory discharge point (i.e. discharged water COP-2), in the middle course of the

74　stream in the zone of total mixing (COP-3) with transect samples points (COP-3.1, COP-3.2

75　and COP-3.3), and two points downstream (COP-4 and COP-5)

3

76   The NPP's liquid discharge started at 2.00 AM and lasted 72 hours. The samplings

77   started 7 hours after the beginning of the discharge (Table 1) to be performed in complete

78   mixing conditions.

79   ***SPM and filtered water sampling for radionuclides analyses***

80   For radionuclides, large volume water samples (from 917 L to 1 313 L) were collected

81   using a high capacity submersible pump and directly passed through 0.50 μm Millipore

82   Milligarde® cartridge filters for particle/solution separation. Ash filters (408°C) were used

83   for SPM radionuclide concentrations. To measure filtered water radionuclide concentration a

84   protocol of radionuclides concentration described in Eyrolle-Boyer *et al.* (2014) that consist

85   in evaporation of 200 L aliquots of filtered waters to dryness (40°C) was used for the Seine

86   River samples.

87

88   ***Dissolved load and Suspended Particulate Matter (SPM) sampling***

89   For major and trace elements, 2 L of grab surface water samples (i.e. depth from 0 to 0.5

90   meter) were sampled, filtered and treated directly in the field. For SPM, large volumes of

91   water river samples (about 20 L of surface water samples) were collected in polyethylene

92   shadow-proof packets for later filtration in the laboratory. For the dissolved load, a first

93   aliquot of the bulk sample was filtered through pre-weighted 0.8 μm glass fiber filters (GFF)

94   for the determination of suspended particulate matter SPM and particular organic carbon

95   (POC) concentrations. During filtration, the first 50 ml of sample solution were discarded,

96   thereby allowing saturation of the filter surface and collecting vessel prior to filtrate recovery.

97   The resulting filtrate was acidified with 85% H_3PO_4 to pH ≤ 2 for dissolved organic carbon

98   (DOC) concentration analyses and stored in amber glass vials. A second aliquot of the bulk

99   sample was filtered through a 0.22 μm acetate-cellulose membrane. One sub sample of the

100   corresponding filtrate was acidified with 15 N distilled nitric acid for further determination of

101 major and trace element concentrations. Another, non-acidified, sub sample of the filtrate was

102 used for determination of anions concentration and alkalinity. After filtration, each collected

103 water sample fraction (i.e. bulk, filtered) was stored in pre-cleaned, acid-washed polyethylene

104 bottles at 4°C until analysis.

105 For the suspended load filtered in the laboratory with a 0.22 µm acetate-cellulose membrane

106 (Millipore) using a Teflon cell and a peristaltic pump towards SPM accumulation. A part of

107 SPM collected on filters was milled using agate mortar and pestle for the X-ray mineralogical

108 composition analysis. Another part aliquot was digested by a tri acid attack (HF, HNO_3, HCl)

109 (Shirai *et al.*, 2015) for the measurements of total major and trace elements concentrations.

110

111 **2.2. Analytical techniques**

112 *2.2.1. Physico-chemical analysis*

113 Water temperature, pH, and conductivity were measured in the field using a WTW 3410

114 Set 2 multi-parameter. Major anion concentrations (Cl^-, F^-, SO_4^{2-}, NO_3^-) were measured by ion

115 chromatography (Thermo Scientific ICS 1100) with an accuracy of 5%. Alkalinity was

116 measured using universal titrator Titrando 809, Metrohm. The dissolved organic carbon

117 (DOC) concentration was determined using a Shimadzu TOC-VCSH analyzer (accuracy

118 1.5%, detection limit 200 µg/L). The particulate organic carbon (POC) was determined using

119 NC Analyser (Flash 2000, Thermo Scientific) with an accuracy of 5%.

120 Total trace and major elements (Na, K, Mg, Ca, Sr, Ba, Fe, Al, Ni) concentrations, in

121 solutions and suspended matter, were determined using a Thermo Fisher ICAP 6200 Duo

122 ICP-OES (accuracy of 5% and detection limit of 2 µg/L). Total trace elements (Mn, Co, Cu,

123 Zn, Ag, Cd, Cs, Pb) with lower concentrations (< 2 µg/L) were measured by Thermo

124 Scientific (Element II) high performance, double focusing ICP-MS (accuracy of 5% and

125 detection limit of 1 ng/L). The SLRS 4 and 5 were used as certified reference materials

126   for those elements.

127   The mineralogical composition of SPM was determined using X-ray diffraction (XRD)

128 analysis on a PANalytical X'pert Pro diffractometer equipped with a multichannel X'celerator

129 detector and using the Co Kα radiation (λ=1.7889 A), in 2θ range of 20-100^0.

130

131   *2.2.2. Radionuclides analysis*

132   The following non stable elements ^{7}Be, ^{60}Co, ^{137}Cs, ^{40}K, ^{228}Ac, ^{234}Th, ^{210}Pb were

133 analyzed by gamma spectroscopy using Ultra low-level well-type HPGe detectors (Canberra)

134 installed in the Modane underground laboratory (France) under 1 700 m of rock. The well-

135 type HPGe detectors are calibrated by Monte Carlo type simulation performed by the codes

136 GeSpeCor (Sima *et al.*, 2001) or Geant3. The simulated model has been validated with the

137 measurements of a standard multi-gamma source in water equivalent resin, contained in 12

138 mL tubes filled up to different heights (1, 3, 6 and 12 mL). The effective germanium crystal

139 volume is 450 cm^3. The resolution of the detector is 1.9 keV at 59 keV; 2.2 keV at 662 keV

140 and 2.4 keV at 1332 keV and its background rate is around 7.2 events/h. MeV in the energy

141 range 30-2700 keV. Additional non stable elements were also measured but will not discussed

142 here, the list is given in the supplementary information section.

143   The discharged water sample (COP-2), was analyzed by gamma spectrometry onto 3 L

144 of the sampling solution by using an ultra-pure germanium gamma spectrometer (Canberra

145 EGPC 42-190-R, P type, relative efficiency 41%) installed at Cadarache.

146

3. Geochemical modeling

148   In the following we will detail the general modeling strategy outlined in Fig. 3.

149 Chemical calculations were made using the Visual Minteq computer code (Gustafsson, 2011,

150 version 3.0 for Windows) which allows to calculate the chemical speciation of elements with

151   inorganic ligands, bindings onto organic compounds by using the NICA-Donnan approach

152   (Benedetti *et al.*, 1995, 1996; Kinniburgh, 1999; Milne *et al.*, 2001, 2003) and trace elements

153   sorption onto hydrous ferric oxide by using the model of Dzombak and Morel (1990) .

154   Adsorption onto clays was accessed by using a non-electrostatic ion exchange model with

155   Gaines-Thomas exchange constants (Appelo and Postma, 2005). For the modeling of Cs

156   adsorption onto clay borders sites including high affinity sites, the 'Fixed-charge site' model

157   was used (Poinssot *et al.*, 1999). For the modeling of sorption onto calcite, a simplified non-

158   electrostatic ion exchange model was used (Zachara et al., 1991; Gaskova et al., 2008, 2009).

159   Input parameters for the simulation of Kd values were: pH, alkalinity, anions, cations, total

160   trace elements (dissolved + SPM), DOC concentrations and the respective amounts of the

161   mineral or organic phases in the SPM (such as POC, hydrous ferric oxide (HFO), clay and

162   calcite) (Fig. 3).

163   In order to describe the interactions between dissolved organic matter and trace

164   elements with the NICA-Donnan model, the knowledge of the nature of the organic matter

165   and its amount is necessary. Humic acid (HA) and fulvic acids (FA) are the two main

166   components used in the NICA-Donnan model as surrogate of the natural organic matter. In

167   natural samples their concentration varies from one sample to another mainly depending on

168   the origin of OM and its degree of degradation. Organic compounds are present in two forms

169   in aquatic samples: the solid form (POC) in SPM, and the so-called dissolved one that may

170   include colloidal components (DOC). According to Tipping (2002), the dissolved organic

171   matter (DOM) is mostly fulvic and the particulate organic matter (POM), which mostly

172   comes from the soils of the watershed, contains more HA. Different compositions with

173   various HA/FA ratios were tested (results not shown) but no significant changes occurred on

174   the log Kd values (i.e. they are within the uncertainties given for the average value of log Rd

in table S3 and S4). Consequently, let us assumed that DOM is 100% composed of FA and

176 POM is 100% composed of HA.

177   The characterization of naturally occurring organic matter (NOM) is expected because

178 the binding capacity of NOM for trace elements most generally depends on NOM quality

179 (Chappaz and Curtis, 2013). Applying an adjustment factor, based on NOM UV-vis quality,

180 Chappaz and Curtis (2013) adjusted the site density for representing the NOM quality but

181 only improved by 30% the goodness of their fits. This gain is of course important for aqueous

182 speciation of the trace elements but it would only lead to a very minor change in log Kd

183 values. NOM's reactivity with trace elements can also be modified due to its own interaction

184 with mineral surfaces. However, such mechanisms are difficult to assess for SPM samples.

185 Therefore, we favored a conservative approach and a ratio of active DOM/DOC and

186 POM/POC of 1.65 has been used as suggested by Sjöstedt et al., (2010).

187   In order to determine the constants related to Cs and Ag complexation with OM we

188 used the approach of Milne (2003) that allows to predict the NICA-Donnan parameter values

189 representative of FA and HA bounds from the first hydrolysis constant (K_{OH}) of the metal by

190 using the correlations. The parameters used for modeling Cs and Ag complexation with OM

191 are those from Milne (2003).

192   Three main types of (hydr)oxides in the SPM were considered: iron, aluminum and

193 manganese (hydr)oxides. Since the concentration of manganese is very low (<10 µg/L), we

194 assumed that trace element adsorption onto manganese oxides is negligible. Lofts and Tipping

195 (2000) showed that the adsorption of metal ions onto aluminum oxides is similar to that

196 generally observed onto iron oxides. Thus, we considered aluminum oxides as iron oxides and

197 associated adsorption properties related to a single mineral grouping these two oxides. In

198 order to describe complexation reactions associated to this generic metal oxide we used the

199 diffuse layer model (DLM) for hydrous ferric oxide (HFO) from Dzombak and Morel (1990)

200   instead of the more robust CD-Music approach proposed by Ponthieu et al., (2006) since

201   spectroscopic speciation data are lacking for the later approach.

202   Clay compounds are represented in the form of nontronite (smectite) with a surface area

203   ranging from 650 to 800 m^2/g and a cation exchange capacity (CEC) of 100 meq/100g

204   (Dejou, 1987). For the adsorption modeling of Cs onto clay borders sites with a high

205   selectivity (Poinssot *et al.*, 1999) we used a fixed charged model with a concentration of

206   borders sites of 0.1 meq/100g. For the adsorption modeling of the others trace element onto

207   clays we used a non-electrostatic ion exchange model with Gaines-Thomas exchange

208   constants (Appelo and Postma, 2005).

209   The nature of adsorption and co-precipitation processes with calcite ($CaCO_3$) surface is

210   complex (Lakshtanov and Stipp, 2007; Wolthers *et al.*, 2008, 2012; Lourino-Cabana *et al.*,

211   2010). Then for the adsorption modeling on calcite we used simplified non-electrostatic ion

212   exchange model with an exchange position density of $3.6 \cdot 10^{-6}$ mol/g and an average surface

213   area of 12.5 m^2/g (Zachara *et al.*, 1991; Gaskova *et al.*, 2008, 2009). The surface of calcite has

214   a near-neutral charge in the range of natural pH values of the Seine River.

215   For a given metal (noted Me), the calculations of saturation index (SI) of the $MeCO_3$

216   show that there is no pure $MeCO_3$ mineral phase precipitation in the Seine River in our

217   conditions. On the other side the SI of calcite ($CaCO_3$), aragonite ($CaCO_3$), dolomite

218   (($Ca,Mg)CO_3$), vaterite ($CaCO_3$) shows the oversaturation of the solution, so $CaCO_3$ could

219   precipitate with associated metals.

220   The contribution in the Kd values of Sr, Co and Ba by co-precipitation with calcite was

221   calculated using the equation (Lourino-Cabana *et al.*, 2010):

222
$$X\text{Me}(predicted) = \frac{\left(\text{Me}^{2+}\right) * (X_{\text{Ca}}) * \text{D}_{Me}^{Calcite}}{(\text{Ca}^{2+})}$$

223   Where (Ca^{2+}) and (Me^{2+}) correspond to the ionic concentrations of Ca^{2+} and Me^{2+},

224   respectively, X_{Ca} and X_{Me} are the Ca and Me molar fractions in the particulate calcite fraction

9

225   at the calcite surface, and $D^{Calcite}_{Me}$ corresponds to distribution coefficient between water and

226   calcite. The $D^{Calcite}_{Me}$ values for Me = Ba, Sr, Ni and Co are 0.06, 0.46, 3.47 and 3.7,

227   respectively (Lourino-Cabana *et al.*,2010).

228   The adsorption of trace element and radionuclide on quartz (SiO_2) was not considered

229   because of its low reactive surface and by the fact that binding constants to quartz are weak

230   compared to those of OM and FeOOH (Schindler and Stumm, 1987; Benedetti *et al.*, 1996).

231

232   **3   Results and discussion**

233   **3.1.   Field data**

234   DOC, POC, ion concentrations, trace and major elements concentrations, alkalinity, pH

235   and conductivity measured in the river during field sampling operations are reported in Tables

236   2 to 4.

237   The studied waters are characteristic of the carbonated watersheds of the Seine River

238   with pH ranging from 8.2 to 8.3 except at the discharge point that displays a pH value of 8.4.

239   Cations concentrations (K^+, Na^+, Mg^{2+}, Ca^{2+}) along the lateral transect sampled are uniform

240   (0.050 − 0.056, 0.24 − 0.26, 0.15 and 2.25 − 2.35 mmol/L, respectively) with systematically

241   higher values for NPP's discharge (0.066, 0.345, 0.19 and 30 mmol/L, respectively). The

242   distributions of major anions concentrations (Cl^-, NO_3^-, SO_4^{2-}) are 0.35-0.38, 0.25-0.26 and

243   0.15-0.21 mmol/L, respectively, with higher values for the NPP's discharge (0.49, 0.34 and

244   1.35 mmol/L, respectively). The alkalinity was of 3.79 ± 0.02 meq/L for the Seine river

245   samples and 2.93 meq/L for the discharge. The DOC concentrations of the Seine river

246   samples cluster around 1.6 ± 0.1 mg/L, a higher value of 2.2 mg/L was measured at the NPP

247   discharge point. Concentrations in the water samples of the NPP's discharge are higher than

248   in upstream and downstream samples (Tables 3 and 4) for: Be (4.2 times), Ba (5.7 times), Ca

249 (1.3), Cd (4.0), Cu (2.5), K (1.3), Mg (1.3), Na (1.4), Ni (1.8), Pb (2), Sr (1.2), Co (1.5), SO_4^{2-}

250 (8.8), Cl^- (1.4), NO_3^- (1.4).

251 SPM concentrations range from 3.5 to 13.5 mg/L without any systematic variations as

252 well as POC concentrations (4.7 – 9.9 %). X-ray analyses for mineral composition showed

253 that SPM from each sample is composed of calcite ($CaCO_3$) at 75 %, quartz (SiO_2) at 20 %

254 and nontronite ($Fe_2H_{10}Na_{0.3}O_{16}Si_4$) and clay (smectite type) at 5 %. XRD analyses did not

255 detect the presence of crystalline iron (hydr)oxide minerals (i.e. < 1%), so iron hydroxide was

256 considered as amorphous. XRD analyses did not detect manganese (hydr)oxide indicating a

257 concentration below 1%.

258 Five percent of SPM is accounted by nontronite, the concentration of amorphous iron

259 hydroxide can be calculated as the difference between the total iron concentration in SPM and

260 the iron concentration in the clay. The amorphous FeOOH concentrations, expressed in mg of

261 Fe per liter of Seine river water, are estimated to vary from 0.1 to 0.2 mg/L in the Seine River

262 samples with the highest concentration observed for the NPP discharge (0.37 mg/L). The Mn

263 concentration in SPM, expressed per liter of water, ranges from 2.6 to 11.4 µg/L

264 The concentrations of artificial radionuclides (^{137}Cs and ^{60}Co) issued from NPP and

265 those of naturally occurring radionuclides ([7]Be, [40]K, [228]Ac, [234]Th and ^{210}Pb) of the Seine River

266 filtrate and SPM samples are reported in Table 3 and Table 4, respectively (see supplementary

267 information for data on other trace elements and radionuclides in Table S1 and S2).

268

269 **3.2. Measured field Rd**

270 Measured field Rd values of stable trace elements and anthropogenic and natural

271 radionuclides are presented in Table S3 and Table S4, respectively and in Figure 4.

272 A literature review, summarized in table S3, shows that average field Rd values of this

273 study are within the range of previously reported values (Alison and Alison, 2005; Sheppard

274 et al., 2009 and Ji et al., 2016). It is, however important to realize that log values tend to

275 minimize differences among samples and sites especially for some trace elements speciation.

276 For instance, if we recompute them in term of percentage of adsorbed metal and dissolved

277 metal similar log Rd will give different distributions. Here for sample COP-1, we give an

278 example for Ba (5% sorbed, 95% dissolved), Cd (41% sorbed and 59% dissolved) and Pb

279 (86% sorbed and 14% dissolved) using the data in tables 2, S2 and S3. Additional

280 calculations, also show that going from COP-1 to COP-2 the Cd field Rd goes from 5.17 to

281 4.74, but concomitantly SPM concentration changes from 4 .26 to 11.26 mg/L of SPM

282 resulting in a much more significant difference in Cd distribution between the two samples

283 (i.e. 20.5% Cd sorbed and 79.5% of Cd dissolved) while for Pb going from log Rd 6.11 to

284 5.88 we obtain 80% adsorbed and 20% dissolved a minor change compared to the distribution

285 in COP-1. This clearly show that Rd to be interpreted needs to be used in combination with

286 more advanced chemical or geochemical modelling concepts based on more detailed physico-

287 chemical parameters, that we put forward in this manuscript. These measures and the

288 geochemical modelling will provide information on the speciation both in the dissolved phase

289 and in the solid phase which is a very important information regarding the bioavailability (and

290 thus toxicity) of the trace metals and radionuclides and that is not available from a Rd

291 parameter.

292

293 In most cases our results show no significant differences between Rds measured at the

294 various sampling points. Indeed, for potassium Log Rd does not vary or very slightly either

295 for its stable isotope (Table S3) or for its main naturally occurring radioactive isotope, namely

296 [40]K (Table S4) without any significant trends between the samples' location. Log Rd values

297 of stable Cs cluster around 6.2 while lower field Rd values were registered for[137]Cs (4.62 –

298 5.37). Log Rd for stable Sr and Ba cluster around 3 and 4.5, respectively (Table S3).

299   Log Rds for Ni, Co and Cu range from 4.35 to 4.91, from 5.10 to 5.81 and from 4.84 to

300   5.35, respectively, and the values increase with increasing distance from NPP's discharge

301   (Table S3) reaching a maximum value in the point COP-5. Average Log Rd of Zn, Cd and Ag

302   were similar and cluster around 5.

303   Log Rd of stable Pb was 5.9 for NPP's discharge and this value is centered at 6.1 for the

304   Seine River samples without any significant trends between the samples' location. Log Rd of

305   ^{210}Pb varies from 4.09, upstream, to 4.94, downstream (Table S4). There is a systematic

306   difference between Rd values of stable Pb and ^{210}Pb continuously produced by the decay of

307   atmospheric ^{222}Rn gas. For the upstream sample this difference is almost two orders of

308   magnitude (Table S3, S4). Usually, this phenomenon can be explained by the different origins

309   of stable and radioactive isotopes: the stable isotope is a constituent of mineral crystal lattices

310   while the radioactive isotope is essentially sorbed onto the surface of particles (FeOOH, MO,

311   clay, etc.) and, therefore, more mobile.

312

313   **3.3.   Comparison between modeled Kd and field Rd**

314   Fig. 5 presents the modeled distribution of trace element and radionuclide on the

315   different surfaces of SPM. Results show that sorption of Cu and Cd is controlled by

316   complexation with particulate OM (99%). Zn, Ni, and Co are adsorbed predominantly on OM

317   (60-75%) and at 25-40% on Fe hydroxide. Pb is adsorbed predominantly on Fe (hydr)oxide

318   (80%) and 20% of particulate Pb is due to its complexation with particulate OM. Cs is

319   absorbed on clay surface at 100 % (Fig 5).

320   Modeled values of Log Kd are also presented in Figure 4 (Table S5). As observed for

321   field Rd values, there are no systematic gaps between modeled Kd values for upstream,

322   downstream and discharge samples.

It is to be noted that in the present work the parameters were not systematically adjusted to obtain the best fit possible between field Rd and Kd. This is simply because it is not the purpose of this paper. It would make no sense to try to have the perfect fit. Doing that, will jeopardize the demonstration that multicomponent models with generic parameters can be of help to simulate real world systems since they give good Kd predictions and that in addition you can get supplementary information on the major species phases controlling the fate of the elements under investigation for a given geochemical ecosystem. What can be useful is to have an idea on the uncertainties of the parameters used here to develop complementary or new approach based on probabilistic generation of parameters' values for given systems to see if the Rd is within the envelope of potential Kd values generated by the methods as shown by Ciffroy and Benedetti , (2018).

Differences induced by filtration will not strongly affect log Rd which are compared on log scale to log Kd since the concentration changes due to different filtration size will affect only by a few % of the bulk concentration the filtrate concentration. Especially for DOM and POM since NOM covers a continuum of sizes that cannot be delimited once for all. Differences observed over several orders of magnitudes like here for log Kd vs log Rd (i.e. 2 to 4) cannot be explained by filtration issues but by affinity constant values for the binding sites. Variations of the amount of matter for the simulated log Kd can modify the Kd value by less than a few tens of % but never by orders of magnitude (Ren et al,2015).

However, the difference between field Rd and modelled Kd values could be related to a kinetic effect rather than a defect from the theoretical assumption of equilibrium. Adsorption and desorption from the particle phase can take several hours and may not be equally fast in time (Ciffroy et al., 2003, Wang et al., 2000).

3.3.1 Elements for which modeled Kd and field Rd are similar (Be, Cd, Cu, Ni, Pb, Zn)

348   Field Rd values for stable Cd, Cu, Ni, Pb and Zn are in good agreement with modeled Kd

349   values (Fig. 4). The minimum values assessed for ^{60}Co and Be[7] are also in good agreement

350   with modeled Kd values, supporting the assumptions made for the modelling.

351

352   3.3.2 Elements for which modeled Kd is higher than measured Rd ([234]Th and ^{210}Pb)

353   There is a difference between stable Pb and [210]Pb: modeled Kd are in good agreement

354   with Rd of stable Pb and not with Rd of [210]Pb. Stable Pb is mostly complexed to SPM and

355   does not take a part of the SPM crystal lattice (Priadi et al, 2011). The difference in Rd values

356   of stable and ^{210}Pb could be explained by the fact that: (1) distribution of ^{210}Pb results from

357   the sorption of this element but also on the sorption of previous elements of the decay chain

358   of [210]Pb (e.g. U, Th, …). These elements (U, Th…) could be more mobile (for example, Kd

359   Th < Kd Pb), consequently more soluble ^{210}Pb could be observed compared to sorbed [210]Pb

360   mobile, and so sorption sites could be different for radioactive and stable Pb (Ayrault et al.,

361   2012). It is also possible that the flux of ^{210}Pb of atmospheric origin to fresh water increased

362   the ^{210}Pb concentration in solution, decreasing the Rd if solid/liquid equilibrium is not

363   reached (Ayrault et al., 2012).

364

365   3.3.3 Elements for which modeled Kd is smaller than measured Rd (Sr, Ba, Ag, Co,

366   Cs and ^{137}Cs)

367   For Co and Cs measured Rd are systematically higher than modeled Kd. The explanations of

368   these differences could be the following ones: (1) Cobalt is incorporated in surface

369   precipitates that are not taken into account in the model (Muray, 1975; Thompson et al., 1999;

370   Siebecker et al., 2014; Gou and Li, 2017); (2) constant of complexation OM-Cs and constant

371   of sorption FeOOH-Cs are not well known (Du et al, 1998; Wang et al., 2000) or missing in

372   the database of the speciation code leading to systematic underestimation of the modeled Kd .

15

373

Modeled Kd values of Th and Ag are systematically smaller than the measured Rd of ^{234}Th and stable Ag. That could be explained by the lack of robustness of the constants of complexation Th-MO used for the modeling. Like in the case of Pb-OM binding constants the Th-OM and Ag-OM NICA-Donnan constants were estimated by Milne (2003) and not experimentally obtained. In addition, Th and Ag correspond to the two extremes cases of this method using a regression line relating K_{OH} and metal ion binding constant, with the first constants of hydrolysis Log K_{OH} of -3.197 and -11.997, respectively (Table S-5). Such "extreme" binding constant values are derived from the linear regression obtained for small range of K_{OH} and thus may explain the underestimation of modeled Kd values (Martin et al., 2020).

Adsorption on calcite modeling in conjunction with modeling of complexation with OM and FeOOH does not show any contribution of calcite in Kd values. So, in perspective for Kd modeling, adsorption on calcite surface could not be considered (Zachara et al., 1991; Uygur and Rimmer, 2000).

However, for elements, like Sr, that are known to be Ca analog further investigation is are necessary by considering the element co-precipitation with calcite. Two simulations were done considering the co-precipitation with a monolayer surface only or on the calcite multilayer surface assuming the co-precipitation on the calcite is a long cycle process where trace element co-precipitate and re-co-precipitate. By considering monolayer co-precipitation no evolution of log Kd value is observed in comparison of log Kd calculated without considering co precipitation (2.40±0.17 and 2.35±0.16 (L/kg), respectively). However, taking into consideration the modeling of Sr multilayer co-precipitation increases log Kd values (3.29±0.16 (L/kg)) in line with the log Rd value measured (Table S3). Not taking into account this phenomenon in log Kd calculation could explain the underestimation of modeled Kd for

16

398   Sr compare to measured Rd (Fig. 4). The same calculations are done for Ba and Co without

399   generating modifications of Kd values suggesting that this phenomenon may not be a major

400   process controlling the Kd values.

401   Similar observations are made when the adsorption onto clay is modeled. In the later,

402   our results show that only Cs is a high selectivity element. Consequently, the modelling of

403   adsorption onto clay is only taken into consideration in the case of Cs.

404   Knowing the trace element distribution between the different sites the current model can

405   be simplified by considering only the major phases and species that control trace element

406   association with solids.

407

408   **3.5 Model fit by adjustment of constitutive fractions**
409

410   Concentrations of stable Cs in SPM are in good agreement with concentrations of stable

411   K, Fe and Al with R^2 of 0.85, 0.90 and 0.89, respectively (Fig. 6A). This could underline

412   adsorption onto clay compounds (nontronite$Fe_2H_{10}Na_{0.3}O_{16}Si_4$) and ionic exchange with K.

413   The concentrations of stable Sr correlate with stable Ca (R^2=0.90), that could indicate the

414   repetitive long-term processes of multilayer co-precipitation with calcite. The concentrations

415   of stable Ni and Co in SPM are in good agreement (R^2=0.99), so we may conclude that these

416   two elements are governed by similar transfer mechanisms and display close adsorption site

417   types. The concentrations of ^{137}Cs in SPM correlate with concentrations of ^{40}K, ^{7}Be, ^{210}Pb and

418   ^{234}Th in SPM with R^2 of 0.99, 0.92, 0.93 and 0.98, respectively (Fig. 6B). We can consider

419   that these radionuclides are concerned by close adsorption sites and behave in the same way

420   in aquatic systems. However, we do not observe any correlations between radionuclides and

421   stable elements. The R^2 of ^{137}Cs with stable K, Fe and Al is of 0.07, 0.11 and 0.007,

422   respectively. We can assume therefore that (1) either the mechanism of the radionuclide (in

423   particular ^{137}Cs) transport is not due to adsorption onto clay compounds (like in the case of

424   stable Cs), or (2) the water sampling, filtration and radionuclide concentrations measurements

425   were performed before equilibrium could be reached. For example, the sorption equilibrium

426   time of ^{137}Cs in the system "water - solid phase" is estimated of 1-3 days (Anikeev and

427   Khristianova, 1973; Behrens et al., 1982; Nosov et al., 2010), whereas our sampling was

428   performed 7-17 h (see Table 1) after the NPP discharge start.

429   Differences of environmental behavior between radiogenic and stable isotopes and

430   consequently the gap between their Kd values are well-known. This was reported by

431   Mundschenk (1996) where measured Rd values for ^{137}Cs in the Rhine river system

432   (SPM/Water and Sediments/Water) were systematically one order of magnitude smaller than

433   stable [133]Cs. Similar results are described in Sheppard *et al.* (2009) where Rd values for

434   radiogenic Sr are lower than the Rd values for geogenic stable Sr. Nosov *et al.* (2010)

435   reported that between two isotopes of one single element of significantly different half-lives,

436   the short-lived one is generally mobile, because it does not associate with the crystalline grid

437   of the mineral while weathering, and because, it does not instantaneously diffuse from the

438   solution to the crystalline structure of the host rock. In the aquatic systems (vs rocks and soils)

439   a ratio between 2 isotopes of one single element (ex. U, Th) may vary from the equilibrium

440   one in ten - hundred times (Nosov *et al.*, 2010) depending on their origin. For example, the

441   most common values of ratios^{234}U/^{238}U and ^{228}Th/^{232}Th concentrations correspond of 1-1.5

442   and 0.9-2.5 for surface waters and 2- 15 and >5.0 for the crystal rocks waters, respectively

443   (Bakhur, 1998).

444

445   **4 Conclusions**

446   The distribution coefficient, Kd, is an integrative representation of complex processes

447   that characterize the partitioning of trace element between solid/liquid and depends on

448   numerous site-specific environmental parameters. In the frame of health and environmental

449   risk assessments dealing with regulatory or accidental radioactive discharges, it is therefore

450   crucial to link Kd values to realistic environmental physico-chemical settings before they are

451   applied to trace element or radionuclides transport modeling in rivers.

452   Here we acquired in-situ solid/liquid ratios (Rd) values for the Seine river by sampling

453   during a NPP's liquid discharge from regulatory operations and compared the data with the

454   results from a geochemical speciation modeling dedicated to Kd calculation.

455   No significant variations of the solid/liquid ratios values were observed in the samples

456   collected in the Seine River during the discharge.

457   The comparison between measured in situ Rd and modelled Kd values for various trace

458   elements and radionuclides lead to identify the main adsorption phases and their dominant

459   transport mechanisms in aquatic systems.

460   The geochemical modeling of Kd for Cu, Zn, Cd, Ni, Co, Pb, Th, Ba, ^{7}Be (with POM

461   and HFO as adsorption phases) and the sequential implementation of additional phases (clay,

462   calcite) show that clay surfaces have to be considered only for Cs because of its high affinity

463   with clay borders and surface basal. For all other trace elements sorption onto clay is not

464   necessary because of its weak exchange constants when compared to complexation constants

465   with organic matter and iron(hydro)oxydes. Considering or not the calcite does not impact

466   significantly their sorption, and consequently their Kd, due to its low surface reactivity and its

467   electro neutrality in natural pH values, and weak constants of exchange TE-calcite by contrast

468   to constants of complexation TE-OM and TE-FeOOH.   For further Kd modeling, we may not

469   take into consideration adsorption on calcite surface.

470   Contrariwise, Sr multilayer co-precipitation shows a significant contribution in final Kd.

471   The adsorption of trace element and radionuclide on quartz (SiO_2) was not considered

472   because of its low reactive surface and by the fact that quartz-binding constants are weak

473   compared to those of OM and FeOOH.

474   This work clearly demonstrate that classical field Rd can be interpreted and completed

475   by advanced chemical or geochemical modelling concepts based on more detailed physico-

476   chemical parameters. In order to test the method relevance further investigations on others

477   nuclearized rivers (ex. Rhône or Loire) with different environmental settings (watershed

478   bedrocks, SPM composition, clay proportion, water discharge, macro-composition, pH, etc.)

479   are necessary.

480

481   **Acknowledgments**

487

References

1. Allison, J. D., and T. L. Allison 2005. Partition coefficients for metals in surface water, soil and waste, Rep. EPA/600/R-05/074, U.S. Environ. Prot. Agency, Off. of Res. and Dev., Washington, D.C.

2. Anikeev V.V., Khristianova L.A. 1973. The distribution coefficients of radionuclides between the solid and liquid phases in the reservoirs, M oscow, Atomizdat (in Russian).

3. Appelo C.A.J., Potma D. 2005. Geochemistry, Groundwater and Pollution, CRC Press 2nd edition, 649 pages

4. Ayrault, S., Roy-Barman, M., Le Cloarec, M-F., Priadi, C., Bonté, P., Göpel, C. 2012 Lead contamination of the Seine River, France: Geochemical implications of a historical perspective, Chemosphere, Volume 87, Issue 8, Pages 902-910,

5. Bakhur, A.E. 1998. Measurement of radioactivity of natural waters and the existing regulatory requirements. Moscow, NPP « Doza » (in Russian).

6. Behrens H., Klotz D. et al. 1982. Comparison of methods for the determination of retention factors of radionuclides in mineral soils // Environmental migration of long-lived radionuclides / IAEA. Vienna, 1982.

7. Benedetti M., Milne C., Kinniburgh D., van Riemsdijk W., Koopal L. 1995. Metal ion binding to humic substances: Application of the non-ideal competitive adsorption model. Environ. Sci. Technol. 29, 446-457.

8. Benedetti M., Van Riemsdijk W. H., Koopal L.K., Kinniburgh D.G., Gooddy D.C., Milne Ch.J. 1996. Metal ion binding by natural organic matter: From the model to the field. Geochim. Cosmochim. Acta 60, 2503-2513.

9. Benes P., Picat P., Cernik M., Quinault J.-M.1992. Kinetics of radionuclide interaction with suspended solids in modeling the migration of radionuclides in rivers. I. parameters for two-steps kinetics. J. Radioanal. Nucl. Chem. 159, 175-186.

10. Benes P., Cernik M., Slavik O. 1994. Modelling of migration of ^{137}Cs accidentally released into a small river. J. Environ. Radioactiv. 22(3), 279-293.

11. Billen G., Garnier J., Mouchel J.-M., Silvestre M. 2007. The Seine system: introduction to a multidisciplinary approach of the functioning of a regional river system. Sci. Total Environ. 375(1-3), 1-12.

12. Bird G.A., Schwartz W. 1997. Distribution coefficients, Kds, for iodide in Canadian shield lake sediments under oxic and anoxic conditions. J. Environ. Radioact. 35, 261-279.

13. Boyer P., Wells, C., Howard, B. 2017. Extended Kd distributions for freshwater environment. J. Environ. Radioactiv. 192, 128-142.

14. Brach-Papa C., Boyer P., Ternat F., Amielh M., Anselmet F. 2005. Characterization and radionuclides sorption of suspended particulate matters in freshwater according to their settling kinetics. Radioprotection, Suppl. 1, 40, S315-S321.

15. Bryan S.E., Tipping E. Hamilton-Taylor J. 2002. Comparison of measured and modelled copper binding by natural organic matter in freshwaters. Comp. Biochem. Phys. C 133, 37-49.

16. Chappaz A. and Curtis P. J. 2013. Integrating Empirically Dissolved Organic Matter Quality for WHAM VI using the DOM Optical Properties: A Case Study of Cu–Al–DOM Interactions. Environ. Sci. Technol 47, 2001–2007.

17. Ciffroy P., Moulin C., Gailhard J. 2000. A model simulating the transport of dissolved and particulate copper in the Seine river. Ecol. Model. 127(2-3), 99-117.

535   18. Ciffroy P., Garnier J. M., Pham M. K. 2001. Kinetics of the adsorption and desorption
536   of radionuclides of Co, Mn, Cs, Fe, Ag and Cd in freshwater systems: experimental
537   and modelling approaches. J. Environ. Radioact. 55(1), 71-91.
538   19. Ciffroy P., Garnier J. M., Benyahya L. 2003. Kinetic partitioning of Co, Mn, Cs, Fe,
539   Ag, Zn and Cd in fresh waters (Loire) mixed with brackish waters (Loire estuary):
540   experimental and modelling approaches. Mar. Pollut. Bull. 46(5), 626-641.
541   20. Ciffroy P., Durrieu G., Garnier, J.M. 2009. Probabilistic distribution coefficients
542   (Kds) in freshwater for radioisotopes of Ag, Am, Ba, Be, Ce, Co, Cs, I, Mn, Pu, Ra,
543   Ru, Sb, Sr and Th: implications for uncertainty analysis of models simulating the
544   transport of radionuclides in rivers. J. Environ. Radioact. 100 (9).
545   21. Ciffroy P. and Benedetti M. (2018) A comprehensive probabilistic approach for
546   integrating natural variability and parametric uncertainty in the prediction of trace
547   metals speciation in surface waters. Environmental Pollution 242, 1087–1097.
548   22. Dejou, J. 1987. La surface spécifique des argiles, sa mesure, relation avec la CEC et
549   son importance agronomique. In : La capacité d'échange cationique et la fertilisation
550   des sols. Amyet Y. ed., 72-83.
551   23. Du, Z., Dong, W.M., Wang, X.K., Liu, H., Tao, V. 1998 Sorption and desorption of
552   radiocesium on calcareous soil and its solid components. J. Radioanal. Nucl. Chem.,
553   231, p. 183
554   24. Dzombak, D.A. and Morel, F.M.M. 1990. Surface complexation modelling: hydrous
555   ferric oxide. Wiley-Interscience, New York.
556   25. EPA 1999. Understanding variation in partition coefficient, Kd, values. Volume II:
557   Review of Geochemistry and Available Kd Values for Cadmium, Caesium,
558   Chromium, Lead, Plutonium, Radon, Strontium, Thorium, Tritium (3H), and
559   Uranium. United States Environmental Protection Agency, Office of Air and
560   Radiation, Report EPA 402-R-99-004B, August 1999.
561   26. Even, S., Billen, G., Bacq, N., Thery, S., Ruelland, D., Garnier, J., Cugier, P., Poulin,
562   M., Blanc, S., Lamy, F., Paffoni, C. 2007. New tools for modelling water quality of
563   hydrosystems: An application in the Seine River basin in the frame of the Water
564   Framework Directive. Science of the Total Environment, 375, 274-291.
565   27. Eyrolle-Boyer, F., Renaud, P., Claval, D., Tournieux, D., Le Dore, F., Blanchet, J.,F.,
566   Loyen, J., Antonelli, C., Cossonnet, C., and Cagnat, X. 2014. Radiological quality
567   Assessment of the Rhône River filtered waters at its lower course in the frame of
568   water production for human consumption - setting Historical and regional
569   perspectives, Radioprotection, 49, 3, 183-193.
570   28. Garnier J.-M., Pham M.K., Ciffroy P. and Martin J.-M. 1997. Kinetics of Trace
571   Element Complexation with Suspended Matter and with Filterable Ligands in
572   Freshwater. *Environ. Sci. Technol.* 31, 1597-1606.
573   29. Gaskova, O.L., Bukaty, M.B. 2008. Sorption of different cations onto clay minerals:
574   Modelling approach with ion exchange and surface complexation. *Physics and*
575   *Chemistry of the Earth 33*, 1050-1055.
576   30. Gaskova, O.L., Bukaty, M.B., Shironosova, G.P., Kabannik, V.G. 2009.
577   Thermodynamic model for sorption of bivalent heavy metals on calcite in natural-
578   technogenicenvironments. *Russian Geology and Geophysics*, 50(2), 87-95.
579   31. Gou, W., Ji, J. & Li, W. 2017 An EXAFS investigation of the mechanism of
580   competitive sorption between Co(II) and Ni(II) at γ-alumina/solution interface. Acta
581   Geochim 36, 462–464. https://doi.org/10.1007/s11631-017-0196-9
582   32. Guérini, M-C., Mouchel, J-M., Meybeck, M., Penven, M-J., Hubert, G., Muxart, T.
583   1998. Le bassin de la Seine: la confrontation du rural et de l'urbain. In: Meybeck, M.,

584   de Marsily, G., Fustec, E., editors. *La Seine en son bassin. Fonctionnement écologique*
585   *d'un système fluvial anthropisé*. Elsevier; p. 29–73.

586   *33.* Gustafsson, J., 2011. Visual MINTEQ ver. 3.0,
587   *http://www2.lwr.kth.se/English/OurSoftware/Vminteq/*

588   34. International Atomic Energy Agency, IAEA 2010. Handbook of Parameter values for
589   the Prediction of Radionuclide Transfer in Terrestrial and Freshwater Environments,
590   Technical Report No 472, Vienna.

591   35. Ji, H., Ding, H., Tang, T., Li, C., Gao, Y., Briki, M. 2016 Chemical composition and
592   transportation characteristic of trace metals in suspended particulate matter collected
593   upstream of a metropolitan drinking water source, Beijing, Journal of Geochemical
594   Exploration, Volume 169, Pages 123-136,
595   https://doi.org/10.1016/j.gexplo.2016.07.018.

596   36. Kinniburgh, D.G., van Riemsdijk, W.H., Koopal, L.K., Borkovec, M., Benedetti,
597   M.F., Avena, M.J. 1999. Ion binding to natural organic matter: competition,
598   heterogeneity, stoichiometry and thermodynamic consistency. Colloids and Surfaces
599   A 151, 147-166.

600   37. Lakshtanov, L. Z., Stipp, S. L. S. 2007. Experimental study of nickel(II) interaction
601   with calcite: Adsorption and coprecipitation. Geochimica et Cosmochimica Acta, 71,
602   3686-3697.

603   38. Lofts S., Tipping E. 2000. Solid-solution metal partitioning in the Humber rivers:
604   application of WHAM and SCAMP.

605   39. Lourino-Cabana, B., Lesven, L., Billon, G., Proix, N., Recourt, P., Ouddane, B.,
606   Fischer, J., Boughriet, A. 2010. Impacts of metal contamination in calcareous waters
607   of Deûle river (France) : water quality and thermodynamic studies on metallic
608   mobility. Water Air and Soil Pollution, 206 (1-4), 187-201. DOI : 10.1007/s11270-
609   009-0095-8.

610   40. Martin L., Simonucci C., Rad S. and Benedetti M. F. 2020 Effect of natural organic
611   matter on thallium and silver speciation. J Environ Sci 93, 185–192.

612   41. Meybeck, M., Horowitz, A. J. and Grosbois, C. 2004. The geochemistry of Seine
613   River Basin particulate matter: distribution of an integrated metal pollution index. *The*
614   *Science of the total environment*, 328(1-3), 219-236.

615   42. Milne, C.J., Kinniburgh, D.G., Tipping, E. 2001. Generic NICADonnan model
616   parameters for proton binding by humic substances. Environmental Science
617   Technology 35, 2049-2059.

618   43. Milne, C.J., Kinniburgh, D.G., Van Riemsdijk, W.H., Tipping, E. 2003. Generic
619   NICA-Donnan model parameters for metal-ion binding by humic substances.
620   Environmental Science Technology 37, 958-971.

621   44. Mundschenk, H. 1996 Occurrence and behaviour of radionuclides in the Moselle
622   River - Part II: Distribution of radionuclides between aqueous phase and suspended
623   matter Journal of Environmental Radioactivity, 30 (3), pp. 215-232

624   45. Murray, J.W. 1975 The interaction of cobalt with hydrous manganese dioxide,
625   Geochimica et Cosmochimica Acta, Volume 39, Issue 5, Pages 635-647,
626   https://doi.org/10.1016/0016-7037(75)90007-1.

627   46. Nosov A. V., Krylov A. L., Kiselev V. P., Kazakov S. V. 2010. Modeling of migration
628   of radioactive substances in surface water.Ed. by R. V. Arutyunyan; Nuclear Safety
629   Institute (IBRAE) RAS.Moscow: Nauka, 253 p.

630   47. O'Connor D. J., Connolly J. P. 1980. The effect of concentration of adsorbing solids
631   on the partition coefficient. *Water Research 14(10),*1517-1523.

632   48. Poinssot, C., Baeyens, B. and Bradbury, M.H. 1999. Experimental and modelling
633   studies of caesium sorption on illite. *Geochim.Cosmochim. Acta 63*, 3217-3227.

634   49. Pokrovsky, O.S., Viers, J., Shirokova, L.S., Shevchenko, V.P., Filipov, A.S., Dupré,
635   B. 2010. Dissolved, suspended, and colloidal fluxes of organic carbon, major and trace
636   elements in the Severnaya Dvina River and its tributary. *Chemical Geology 273*(1-2),
637   136-149.
638   50. Ponthieu M., Juillot F. van RiemsdijkW.H. and Benedetti M.F. 2006. Metal ion
639   binding to iron oxides. *Geochimica et Cosmochimica Acta, 70*, 2679-2698.
640   51. Priadi C., Ayrault S., Pacini S. and Bonte P. 2011 Urbanization impact on metals
641   mobility in riverine suspended sediment: Role of metal oxides. International Journal
642   of Environmental Science and Technology 8, 1–18.
643   52. Radovanovic, H., Koelmans, A.A. 1998. Prediction of in situtrace metal distribution
644   coefficients for suspended solids in natural waters. *Environ. Sci. Technol.* 32, 753-759.
645   53. Ren Z.-L., Tella M., Bravin M. N., Comans R. N. J., Dai J., Garnier J.-M., Sivry Y.,
646   Doelsch E., Straathof A. and Benedetti M. F. (2015) Effect of dissolved organic
647   matter composition on metal speciation in soil solutions. Chemical Geology 398, 61–
648   69.
649   54. Roy, S., Gaillardet, J., and Allègre, C.J. 1999. Geochemistry of dissolved and
650   suspended loads of the Seine River, France: anthropogenic impact, carbonate and
651   silicate weathering. Geochimica et Cosmochimica Acta, 63(9), 1277-1292.
652   55. Schindler P. W. and Stumm W. 1987. The Surface chemistry of oxides, hydroxides
653   and oxide minerals. In Aquatic Surface Chemistry (ed. W. Stumm). John Wiley and
654   Sons, pp. 83–107.
655   56. Sheppard, S., Long, J., Sanipelli, B., Sohlenius, G. 2009. Solid/liquid partition
656   coefficients (Kd) for selected soils and sediments at Forsmark and Laxemar-
657   Simpevarp. SKB rapport R-09-27, SvenskKarnbranslehantering AB, 78p.

658   57. Shirai N., Toktaganov M., Takahashi H., Yokozuka Y., Sekimoto S. and Ebihara M.
659   2015 Multielemental analysis of Korean geological reference samples by INAA, ICP-
660   AES and ICP-MS. J. Radioanal Nucl Chem 303:1367–1374
661   58. Sibley, T.H., Wurtz, E.A., Alberts, J.J. 1986. Partition coefficients for [244]Cm on
662   freshwater and estuarine sediments. Journal of Environmental Radioactivity, 3(3),
663   203-217, DOI: 10.1016/0265-931X(86)90026-3
664   59. Siebecker, M., Li, W., Khalid, S. et al. 2014 Real-time QEXAFS spectroscopy
665   measures rapid precipitate formation at the mineral–water interface. Nat Commun 5,
666   5003. https://doi.org/10.1038/ncomms6003

667   60. Sima, O., Arnold, D. & Dovlete, C. GESPECOR: A versatile tool in gamma-ray
668   spectrometry.Journal of Radioanalytical and Nuclear Chemistry 248, 359–364 (2001).
669   61. Sjöstedt, C.S., Gustafsson, J.P. and Köhler, S.J. 2010. Chemical equilibrium modeling
670   of organic acids, pH, aluminum and iron in Swedish surface waters. *Environ. Sci.*
671   *Technol. 44*, 8587-8593.
672   62. Thompson, H. A., Parks, G. A. and Brown, G. E. 1999 Dynamic interactions of
673   dissolution, surface adsorption, and precipitation in an aging cobalt(II)-clay-water
674   system, Geochimica et Cosmochimica Acta, Volume 63, Issues 11–12, Pages 1767-
675   1779, https://doi.org/10.1016/S0016-7037(99)00125-8.
676   63. Tipping, E. 2002. Cation binding by humic substances. Cambridge University Press,
677   Cambridge, 442 p.
678   64. Tipping, E., Lofts, S., & Lawlor, A. J. 1998. Modeling the chemical speciation of
679   trace metals in the surface waters of the Humber system. *Science of the Total*
680   *Environment*, 210-211, 63-77.

681   65. Tomczak, W., Boyer, P., Krimissa, M., & Radakovitch, O. 2019. Kd distributions in
682   freshwater systems as a function of material type, mass volume ratio, dissolved
683   organic carbon and pH. Applied Geochemistry, 105, 68-77.
684   66. Uygur, V. and Rimmer, D.L. 2000 Reactions of zinc with iron-oxide coated calcite
685   surfaces at alkaline pH. European Journal of Soil Science, 51: 511-516.
686   doi:10.1046/j.1365-2389.2000.00318.x
687   67. Vesely, J., Majer, V., Kucera, J., and Havranek, V. 2001. Solid-water partitioning of
688   elements in Czech freshwaters. *Applied Geochemistry,* 16, 437-450.
689   68. Wang, X., Dong,W., Li, Z., Du, J., Tao, Z. 2000 Sorption and desorption of
690   radiocesium on red earth and its solid components: relative contribution and
691   hysteresis, Applied Radiation and Isotopes,Volume 52, Issue 4, Pages 813-819,
692   69. Wolthers, M., Charlet, L., & Van Cappellen, P. 2008. The surface chemistry of
693   divalent metal carbonate minerals; a critical assessment of surface charge and
694   potential data using the charge distribution multi-site ion complexation model.
695   *American Journal of Science* 308, 905-941.
696   70. Wolthers, M., Nehrke, G., Gustafsson, J. P., & Van Cappellen, P. 2012. Calcite
697   growth kinetics: Modeling the effect of solution stoichiometry. Geochimica et
698   Cosmochimica Acta, 77, 121-134.
699   71. Xue, H.B., Gachter, R., Sigg, L., 1997. Comparison of Cu and Zn in eutrophic lakes
700   with oxic and anoxic hypolimnion. *Aquat. Sci.* 59, 176-189.
701   72. Zachara, J. M., Cowan, C. E.,Resch, C. T. 1991. Sorption of divalent metals on
702   calcite. Geochimica et Cosmochimica Acta 55, 1549-1562.
703   73. Zhao, L. X., & Hou, W. G. 2012. The effect of sorbent concentration on the partition
704   coefficient of pollutants between aqueous and particulate phases. *Colloids and*
705   *Surfaces A: Physicochemical and Engineering Aspects*, 396, 29-34.
706
707

Figure Captions:

Figure 1. The sampling sites location along the Seine River. Samples were taken at depth between 0 and 0.5 meters.

Figure 2. Geochemical and radionuclide analysis conducted in the field and in the laboratory. The full data set is given in supplementary material. Water constituents taken into account to obtain model Kd values to be compared to field Rd retrieved from the geochemical analysis.

Figure 3. Modelling workflow used to compute trace elements and radionuclides speciation and derived model Kd. For each element the generic data bases of models' parameter were used. Please refer to given references for more detailed information.

Figure 4. Modelled log Kd versus field log Rd for trace elements and radionuclides. The * indicates minimum field log Rd values. Error bars are included in the symbols.

Figure 5. Modelled trace elements distribution among the different surfaces of the suspended particulate matter.

Figure 6. Panel A showing the correlations between the stable K, Fe and Al concentrations and stable Cs concentration. Panel B showing the correlations between concentrations of [7]Be, [40]K, ^{210}Pb, [234]Th and ^{137}Cs in the suspended particulate matter.
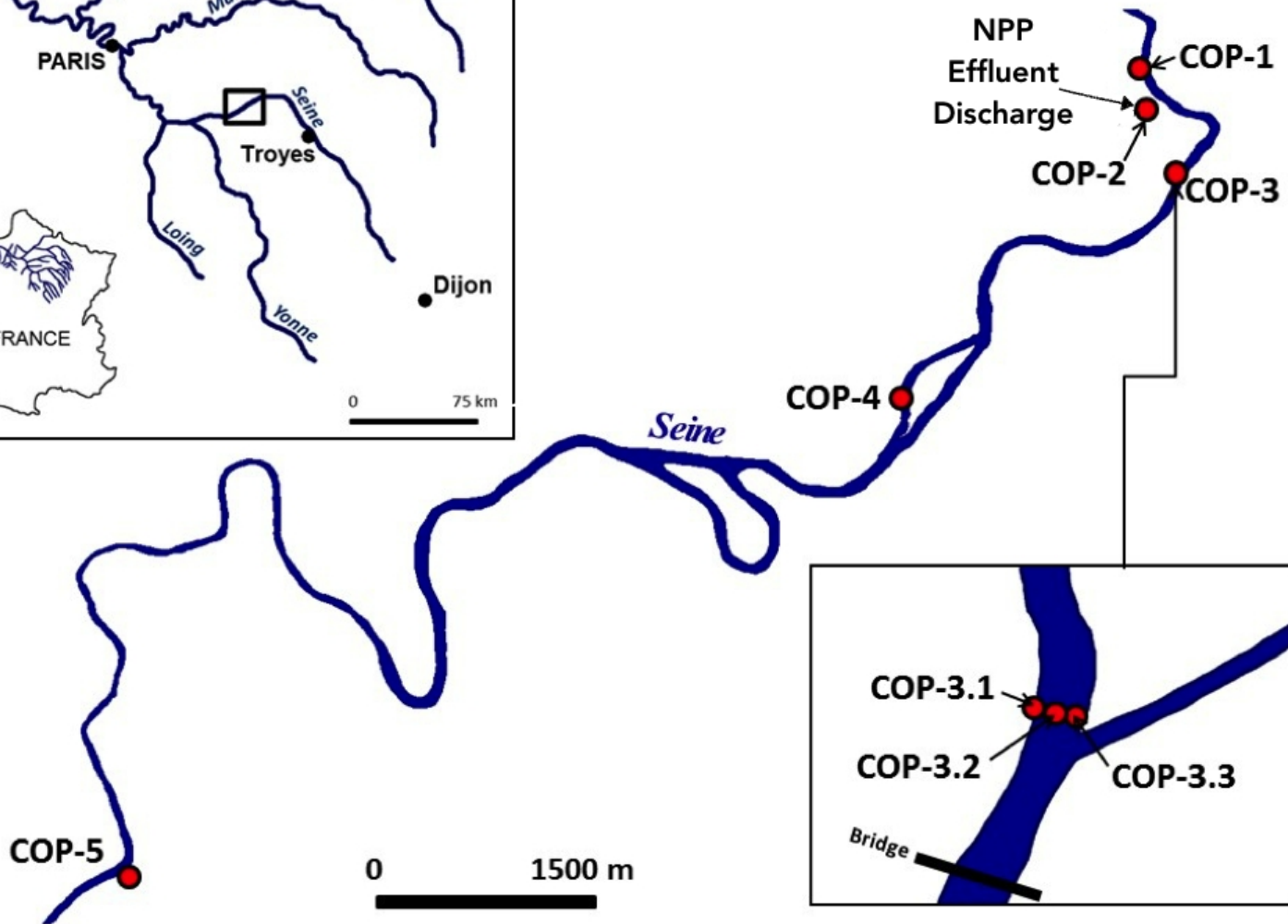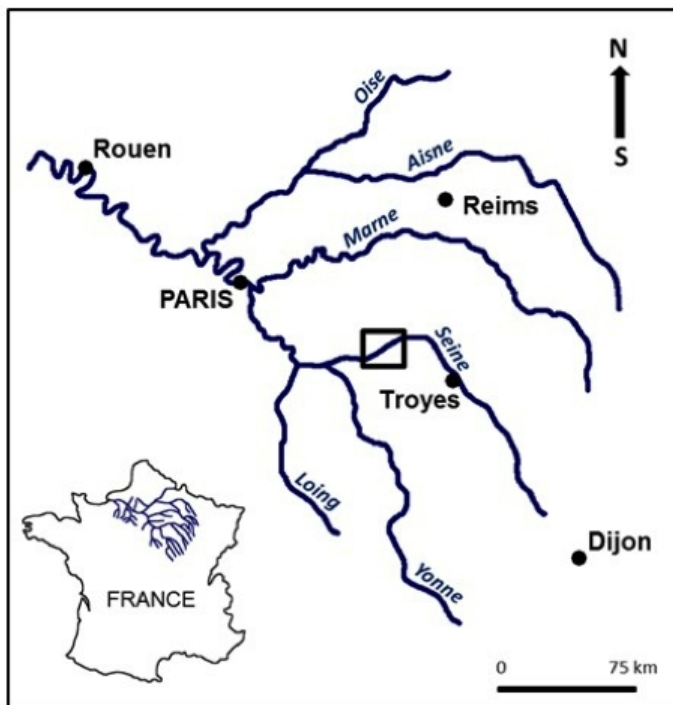
Geochemical Analysis:
Field Data: T°, pH, Conductivity, $[O_2]$, Alkalinity.

Laboratory Measurements:
Dissolved Fraction: [Anions], [Cations], [DOC], [Trace Elements]
Suspended Matter : [SPM], [POC], [Trace Elements], Mineralogy

Input   Data

Radionuclide Analysis:
Dissolved Fraction: activity of RN,
Suspended Matter : activity of RN

Speciation Modelling

Inorganic Complexes

Colloids :POM, Clay, (Hydr)oxides, Carbonates

Dissolved

Particulate

H_2O H_2O Me OH_2 OH_2 H_2O

Macromolecular Complexes : DOM

Living organisms Not include here

Field **Rd** (Stable Elements)   ? =   Field **Rd** (Natural RN)
Field **Rd** (Artificial RN)   ? =   Modelled **Kd** (Stable Elements)
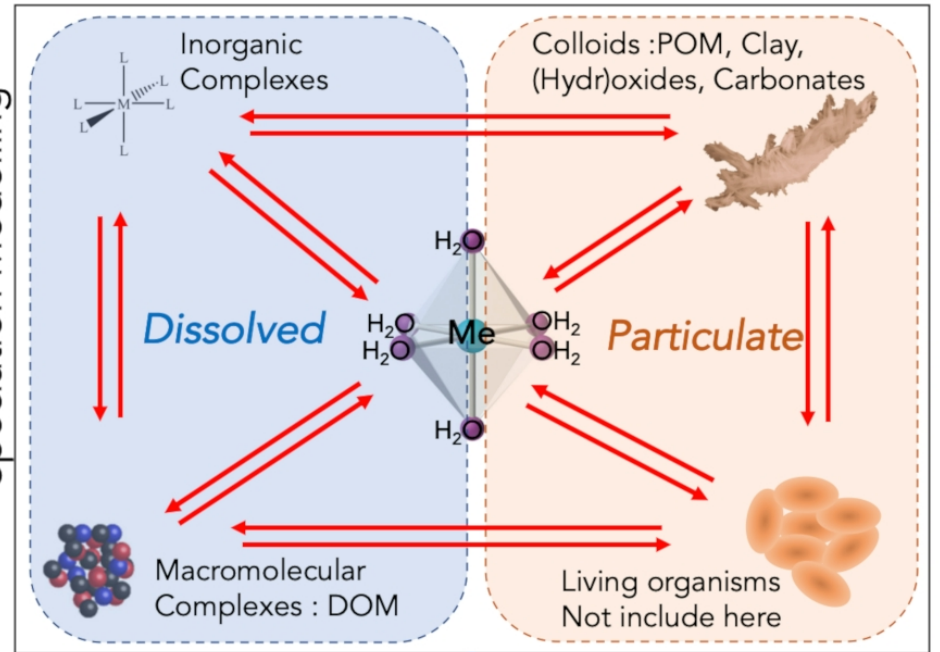
Input Data:
T°, pH, [O₂], Alkalinity.

Dissolved Fraction: [Anions], [Cations], [DOC], [Trace Elements]

Suspended Matter : [SPM], [POC], [Trace Elements], Mineralogy

Geochemical Speciation Modelling

Output Data:
Free ionic species : Me^{z+}
Inorganic Complexes : MeL_n
Bound to DOM : Me-DOM
Bound to POM : Me-POM
Sorbed to (Hydr)oxides : Me-HFO
Sorbed to Clays : Me-Clay
Sorbed to Calcite : $Me\text{-}CaCO_3$

Colloids :

POM: NICA-Donnan Model, (Benedetti et al., 1996 - Kinniburgh et al., 1999) With generic parameters from Milnes et al., (2001, 2003)

Clay: Ion exchange model Gaines Thomas (Appelo & Postma, 2005) Clay: For Cs only, Fixed Charge site model (Poinssot et al., 1999)

(Hydr)oxides: Surface complexation model (Dzomback & Morel, 1990)

Carbonates: Ion exchange model (Zachara et al., 1999 - Gaskova et al., 2009)

Particulate

DOM: NICA-Donnan Model, (Benedetti et al., 1996 - Kinniburgh et al., 1999) With generic parameters from Milnes et al., (2001, 2003)
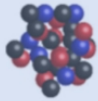
Inorganic Complexes Visual Minteq data base.

Dissolved

Modelled Kd (Stable Elements)

B

R² = 0.99   K
R² = 0.92   Be
R² = 0.92   Pb
R² = 0.98   Th
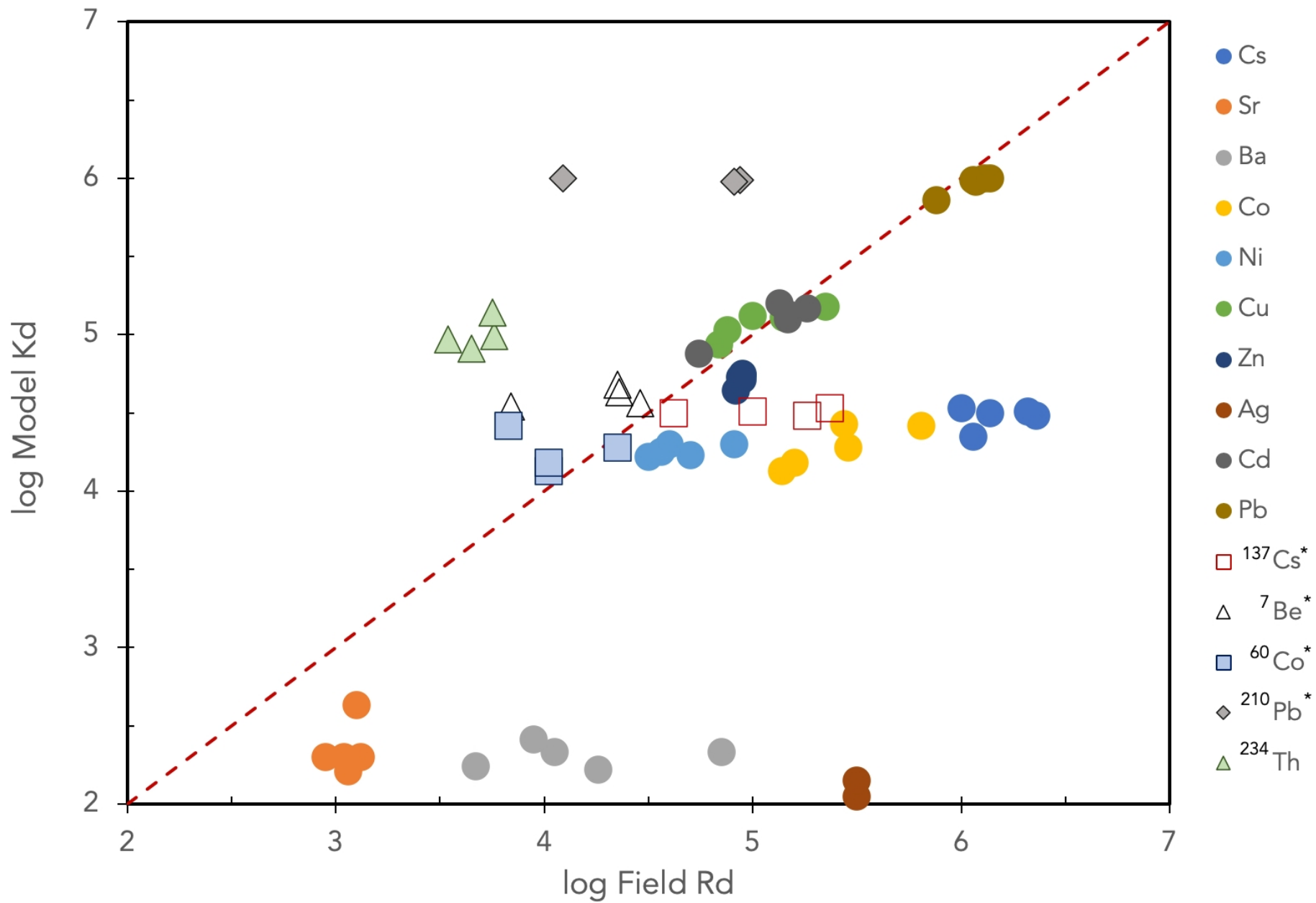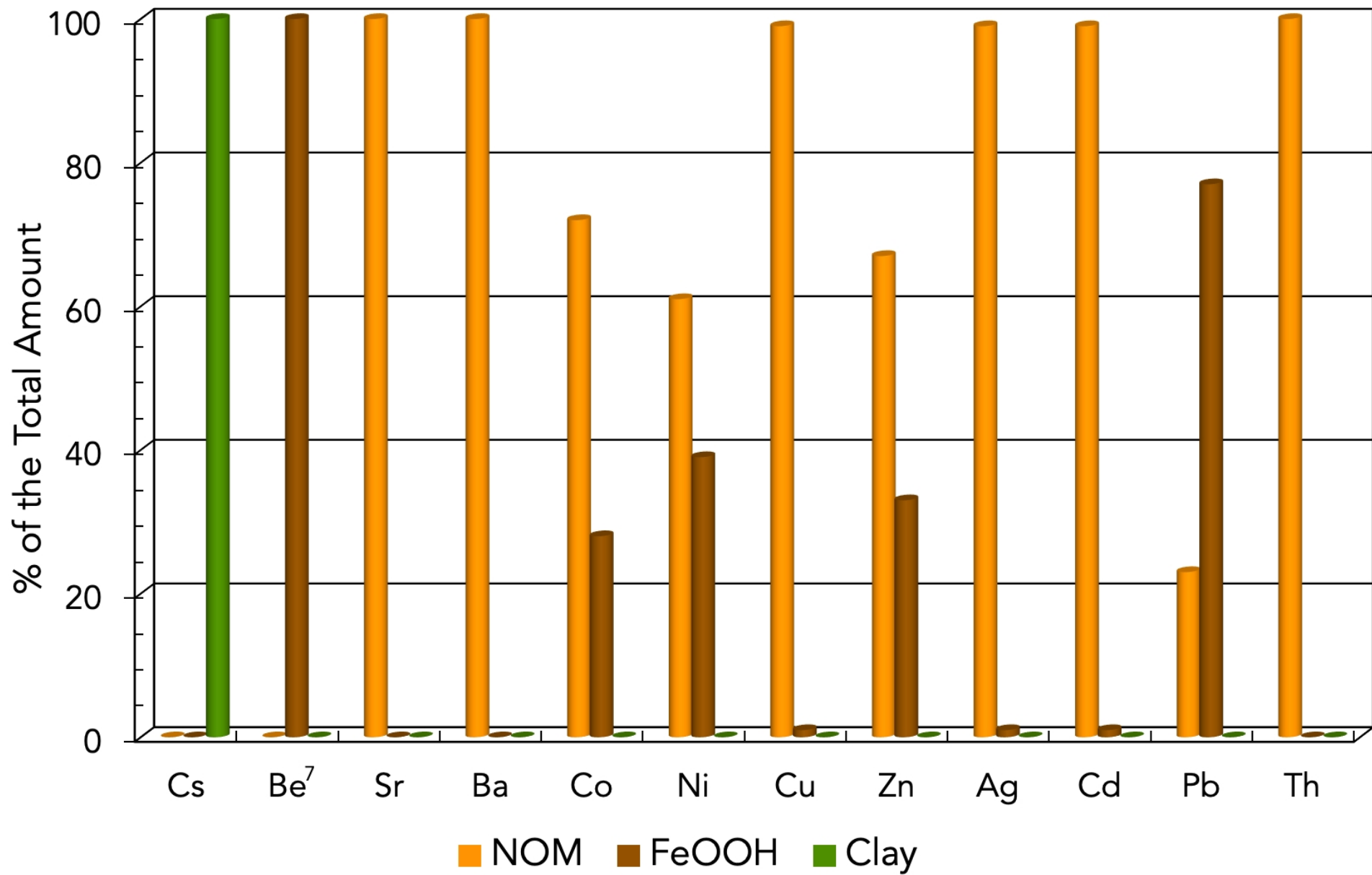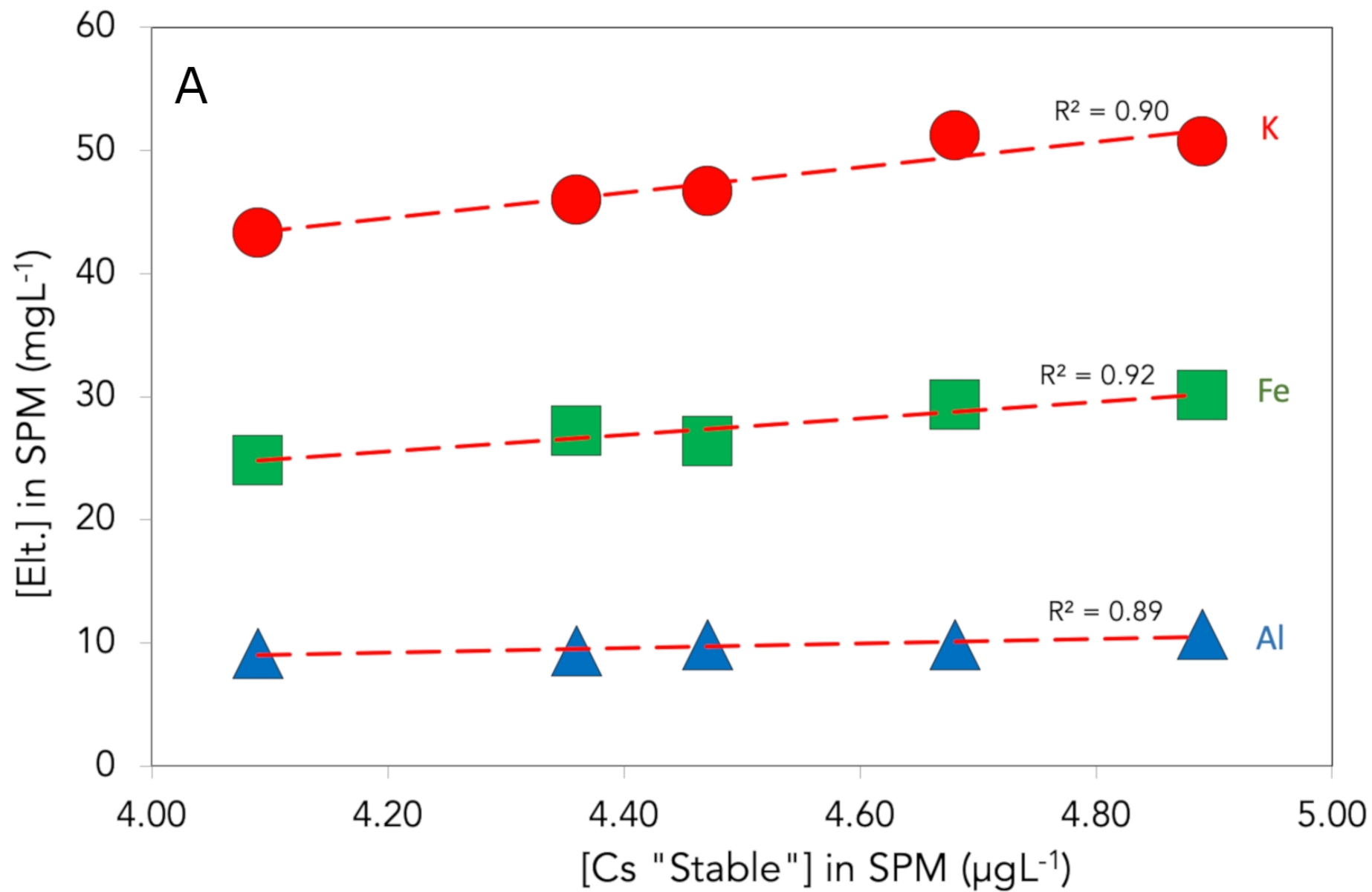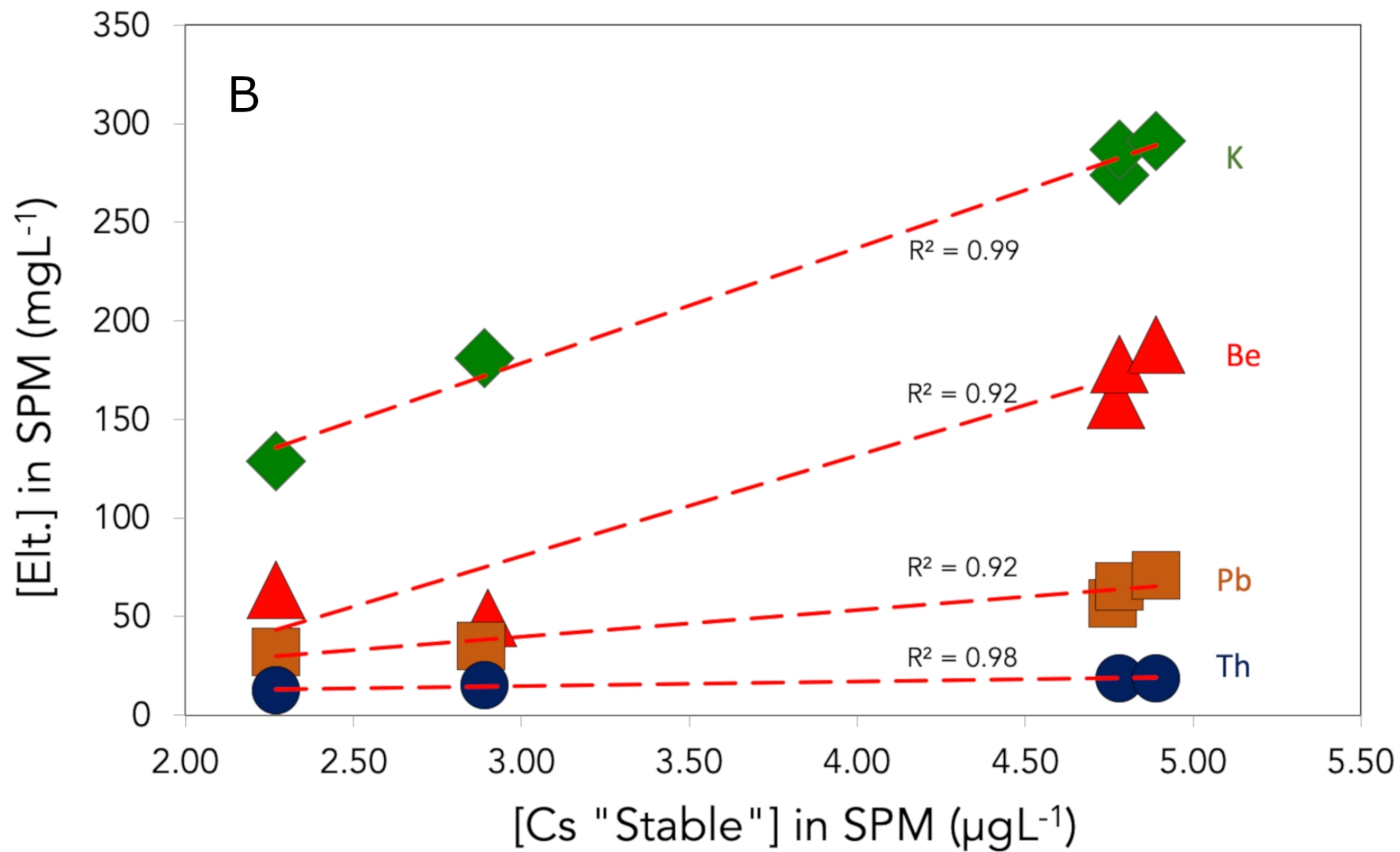
TABLES

Table 1. List of collected water samples

Sample point	Description	Time of sampling from start of NPP discharge, hours
COP-1	Upstream point, 250 m upstream the discharge	7
COP-2	Effluent Discharge pipe	8
COP-3	Middle course of the river, zone of full mix, 1 km downstream the Discharge	10.5
COP-3.1	Transect point 1, right waterside, 65 m downstream COP-3	10.5
COP-3.2	Transect point 2, middle flow, 65 m downstream COP-3	11.5
COP-3.3	Transect point 3, left waterside, 65 m downstream COP-3	13
COP-4	Downstream, 4.05 km downstream the Discharge	15
COP-5	Downstream, 14.15 km downstream the Discharge	17

Table 2. Geochemical characteristics of the sampling points (August 2013).

	COP-1	COP-2	COP-3.1	COP-3.2	COP-3.3	COP-4	COP-5
T, °C	20.2	25.2	21.1	21.1	21.4	21.7	21.7
pH	8.21	8.41	8.26	8.27	8.26	8.28	8.32
χ, µS/cm	484	565	493	500	503	500	493
O_2, %	94	100	98	99	100	100	100
TDS, mg/L	8.47	8.37	8.71	8.81	8.82	8.69	9.03
Alkalinity, µeq/L	3820	2934	3787	3787	3787	3770	3770
[DOC], mg/L	1.61	2.19	1.59	1.59	1.64	1.66	1.67
[F^-], µMol/L	5.36	6.60	6.30	5.83	5.96	5.38	6.41
[Cl^-], µMol/L	354	495	369	368	371	378	380
[NO_3^-], µMol/L	251	341	255	253	253	260	259
[SO_4^{2-}], µMol/L	154	1355	206	205	205	207	210
[K^+], µmol/L	50	66	51	50	51	52	56
[Na^+], µmol/L	241	345	249	250	256	256	261
[Mg^{2+}], µmol/L	154	191	153	154	156	154	155
[Ca^{2+}], µmol/L	2270	2970	2310	2313	2358	2333	2310
[SPM], mg/L	4.67	11.26	3.72	3.50	13.53	7.11	3.65
[POC], mg/L	0.36	1.11	0.37	0.33	0.64	0.47	0.27
[K]$_{SPM}$, g/kg	9.95	10.8	9.4	10.1	8.23	9.86	9.5
[Ca]$_{SPM}$, g/kg	205	174	184	190	174	194	206
[Mg]$_{SPM}$, g/kg	4.62	4.91	4.33	4.67	3.77	4.82	4.82
[Fe]$_{SPM}$, g/kg	26.8	30.5	25.1	28.2	22.3	29.9	27.7
[Al]$_{SPM}$, g/kg	46.5	50.6	42.9	49.0	38.4	51.2	45.9
[Mn]$_{SPM}$, g/kg	0.715	1.02	0.71	0.86	0.72	1.03	0.81
Calcite, % in SPM	75	75	75	75	75	75	75
Quartz, % in SPM	20	20	20	20	20	20	20
Clays, % in SPM	5	5	5	5	5	5	5

Table 3. Major and trace elements (µg/L) and radionuclides (Bq/L) concentrations in the dissolved load.

	COP-1	COP-2	COP-3	COP-3.1	COP-3.2	COP-3.3	COP-4	COP-5	
Cs	0.0047	0.00442	-	0.00412	0.00215	0.00201	0.00211	0.00217	
Sr	224	275	-	223	224	227	227	228	
Ba	16.31	91.13	-	17	16.51	16.68	16.55	16.93	
Co	0.047	0.0726	-	0.0463	0.047	0.0475	0.0476	0.046	
Ni	0.95	1.74	-	1.1	1.2	1.3	1.18	1.12	
Cu	0.676	1.79	-	0.594	0.461	0.4	0.462	0.405	
Zn	2.05	3.49	-	2.84	3.51	3.39	3.49	2.54	
Ag	<0.001	<0.001	-	0.002	<0.001	<0.001	0.002	<0.001	
Cd	0.0026	0.00832	-	0.00411	0.00164	0.00176	0.0031	0.00201	
Pb	0.018	0.0372	-	0.0236	0.0169	0.0167	0.0212	0.0183	
									$T_{1/2}$
^{137}Cs	<0.000021	<0.03	<0.000114	-	-	-	<0.000027	<0.000023	30.17 years
^{7}Be	0.0071	<0.5	0.0062	-	-	-	0.0081	0.0091	53.3 days
^{60}Co	<0.000043	<0.03	<0.000071	-	-	-	<0.000059	<0.000058	5.27 years
^{210}Pb	0.0048	<7.2	0.00078	-	-	-	0.00091	<0.0013	22.3 years
^{234}Th	0.0033	<7.6	0.0034	-	-	-	0.0042	0.0036	24.1 days

Table 4. Major and trace elements (mg/kg $_{dry}$) and radionuclides (Bq/kg $_{dry}$) concentrations in the suspended particulate matter.

	COP-1	COP-2	COP-3	COP-3.1	COP-3.2	COP-3.3	COP-4	COP-5
Cs	4.67	5.09	-	4.21	4.90	3.77	4.88	4.56
Sr	283	244	-	257	265	238	263	300
Ba	181	428	-	175	183	162	301	1200
Co	6.49	20.0	-	6.25	7.51	5.96	13.9	29.7
Ni	34	69	-	34	36	29	59	92
Cu	51	124	-	53	72	55	65	90
Zn	183	307	-	293	319	263	287	228
Ag	0.446	0.710	-	0.592	0.553	0.402	0.592	0.936
Cd	0.381	0.459	-	0.447	0.412	0.343	0.460	0.366
Pb	23	28	-	25	25	21	25	25
^{137}Cs	4.78	2.9*	4.79	-	-	-	4.89	2.27
^{7}Be	159.9	49*	176.9	-	-	-	187.2	62.25
^{60}Co	<0.46	<0.26*	0.74	-	-	-	1.32	0.39
^{210}Pb	59.7	38*	67.3	-	-	-	73.4	34.6
^{234}Th	19.3	15*	19.35	-	-	-	18.8	12.45

* Suspended sediments from the pump (average sample of 1 month)

Declaration of interests

☒ The authors declare that they have no known competing financial interests or personal relationships that could have appeared to influence the work reported in this paper.

☐The authors declare the following financial interests/personal relationships which may be considered as potential competing interests:

Solid/liquid ratios of trace elements and radionuclides during a Nuclear Power Plant liquid discharge in the Seine River: Field measurements vs geochemical modelling

Svetlana M. Ilina[1], Laura Marang[2], Beatriz Lourino-Cabana[2], Frédérique Eyrolle[3], Patrick Boyer[3], Frederic Coppin[3], Yann Sivry[1], Alexandre Gélabert[1], Marc F. Benedetti[1*]

[1]Université de Paris, Institut de physique du globe de Paris, CNRS, IGN, F-75238 Paris, France

[2] EDF R&D LNHE - Laboratoire National d'Hydraulique et Environnement, 6 quai Watier, 78401 Chatou, France

[3] Institut de Radioprotection et de Sûreté Nucléaire (IRSN) PSE-ENV/SRTE, Cadarache, Saint Paul Lez Durance, 11315, France

- Corresponding author
- Professor : Marc F. Benedetti
- Université de Paris, Institut de physique du globe de Paris, CNRS, IGN,
- 1 rue Jussieu F-75238 Paris, France
- E-mail address: *benedetti@ipgp.fr*

1- RN analysis

The following additional radionuclides were also measured ^{110m}Ag, ^{241}Am, ^{57}Co, ^{58}Co, ^{134}Cs, ^{154}Eu, ^{54}Mn, ^{22}Na, ^{106}Rh, ^{124}Sb, ^{125}Sb, were analyzed using Ultra low-level well-type HPGe detectors (Canberra) installed in the Modane underground laboratory (France) under 1 700 m of rock. The well-type HPGe detectors are calibrated by Monte Carlo type simulation performed by the codes GeSpeCor (Sima *et al.*, 2001) or Geant3. The simulated model has been validated with the measurements of a standard multi-gamma source in water equivalent resin, contained in 12 mL tubes filled up to different heights (1, 3, 6 and 12 mL). The effective germanium crystal volume is 450 cm^3. The resolution of the detector is 1.9 keV at 59 keV; 2.2 keV at 662 keV and 2.4 keV at 1332 keV and its background rate is around 7.2 events/h. MeV in the energy range 30-2700 keV.

For ^{63}Ni analyses, samples were dissolved together with a known amount of stable nickel used as carrier and chemical yield. Solution were prepared in citrate medium at pH 8 and then passed on a chromatographic column containing dimethylglyoxime (DMG) to form a Ni-DMG complex. After washing the column, the nickel is eluted with 3 M HNO_3. It is then precipitated with DMG again. After filtration and washing the precipitate, the Ni-DMG complex is oxidized to NiO by calcination oven at 500°C. The obtained oxide was dissolved in a mixture HNO_3/HCl. The solution is evaporated and the residue taken up in 6 ml of 0.1M HCl. An aliquot of the final solution is taken for the measurement of total nickel by ICP- AES for the determination of chemical yield and 4 ml were counted by liquid scintillation to determine the ^{63}Ni activity (from Holm *et al.*, 1992). Holm E., Rots P. and Skwarzec B. 1992. Radioanalytical Studies of Fallout 63Ni. Appl. Radiat. Isot. 43(1/2), 371-376.

2- Results

Despite a protocol designed to decrease the quantification limits, the concentrations of ^{110m}Ag, ^{58}Co and ^{63}Ni measured in the effluent discharge pipe and in the filtered water and SPM sampled in the Seine River display values below the quantification capabilities. In situ Kd values for these RN's from our field experiment are therefore unavailable. However, the concentrations of ^{137}Cs and ^{60}Co are below the quantification limits in the filtered waters but above the quantification limits in SPM so it is possible to estimate minimum Kd values for ^{137}Cs and ^{60}Co: Kd_{min} = [RN]SPM / [RN] w, detection limit.

All artificial RNs concentrations from the discharge were below the limit of quantification (Tables S-2 and S-3) even though suitable analytical tools were used for their detection.

3- Additional tables

Table S-1. Major and trace elements (µg/L) and radionuclides (Bq/L) concentrations in the dissolved fraction (august 2013).

	COP-1	COP-2	COP-3	COP-3.1	COP-3.2	COP-3.3	COP-4	COP-5	
Na	5506	7914	-	5702	5727	5871	5868	5968	
K	1941	2571	-	1986	1940	1993	2033	2192	
Cs	0.00470	0.00442	-	0.00412	0.00215	0.00201	0.00211	0.00217	
Mg	3743	4643	-	3720	3735	3789	3751	3774	
Ca	90787	118794	-	92449	92522	94331	93335	92361	
Sr	224	275	-	223	224	227	227	228	
Ba	16.31	91.13	-	17	16.51	16.68	16.55	16.93	
Al	1.54	1.49	-	0.652	2.02	<0.2	<0.2	<0.2	
Mn	1.20	0.925	-	1.62	1.70	1.93	1.87	1.82	
Fe	4.75	4.34	-	2.60	3.66	3.85	3.58	4.16	
Co	0.0470	0.0726	-	0.0463	0.0470	0.0475	0.0476	0.0460	
Ni	0.950	1.74	-	1.10	1.20	1.30	1.18	1.12	
Cu	0.676	1.79	-	0.594	0.461	0.400	0.462	0.405	
Zn	2.05	3.49	-	2.84	3.51	3.39	3.49	2.54	
Ag	<0.001	<0.001	-	0.002	<0.001	<0.001	0.002	<0.001	
Cd	0.00260	0.00832	-	0.00411	0.00164	0.00176	0.00310	0.00201	
Sb	0.0745	0.112	-	0.0728	0.0730	0.0736	0.0737	0.0783	
Pb	0.0180	0.0372	-	0.0236	0.0169	0.0167	0.0212	0.0183	
									$T_{1/2}$
^{40}K	0.051	<0.4	0.055	-	-	-	0.056	0.068	$1.3 \cdot 10^9$ years
^{137}Cs	<0.000021	<0.03	<0.000114	-	-	-	<0.000027	<0.000023	30.17 years
^{7}Be	0.0071	<0.5	0.0062	-	-	-	0.0081	0.0091	53.3 days
^{60}Co	<0.000043	<0.03	<0.000071	-	-	-	<0.000059	<0.000058	5.27 years
^{210}Pb	0.0048	<7.2	0.00078	-	-	-	0.00091	<0.0013	22.3 years
^{228}Ac	0.00069	<0.1	0.00059	-	-	-	0.00064	0.00076	6.15 hours
^{234}Th	0.0033	<7.6	0.0034	-	-	-	0.0042	0.0036	24.1 days

Table S-2. Major and trace elements (mg/kg $_{dry}$) and radionuclides (Bq/kg $_{dry}$) concentrations in suspended particulate matter (august 2013).

	COP-1	COP-2	COP-3	COP-3.1	COP-3.2	COP-3.3	COP-4	COP-5
Na	1495	877	-	850	670	661	730	1264
K	9955	10822	-	9395	10085	8229	9862	9496
Cs	4.67	5.09	-	4.21	4.90	3.77	4.88	4.56
Mg	4616	4906	-	4325	4669	3773	4819	4814
Ca	204489	173816	-	183974	189586	173620	193830	206170
Sr	283	244	-	257	265	238	263	300
Ba	181	428	-	175	183	162	301	1200
Al	46509	50584	-	42859	49011	38437	51174	45929
Mn	715	1016	-	709	861	724	1030	805
Fe	26812	30574	-	25141	28229	22324	29889	27709
Co	6.49	20.0	-	6.25	7.51	5.96	13.9	29.7
Ni	34	69	-	34	36	29	59	92
Cu	51	124	-	53	72	55	65	90
Zn	183	307	-	293	319	263	287	228
Ag	0.446	0.710	-	0.592	0.553	0.402	0.592	0.936
Cd	0.381	0.459	-	0.447	0.412	0.343	0.460	0.366
Sb	0.577	1.05	-	0.746	0.541	0.491	0.516	0.509
Pb	23	28	-	25	25	21	25	25
^{40}K	275.7	181*	285.7	-	-	-	291.0	128.5
^{137}Cs	4.78	2.9*	4.79	-	-	-	4.89	2.27
^{7}Be	159.9	49*	176.9	-	-	-	187.2	62.25
^{60}Co	<0.46	<0.26*	0.74	-	-	-	1.32	0.39
^{210}Pb	59.7	38*	67.3	-	-	-	73.4	34.6
^{228}Ac	18.4	17*	19.35	-	-	-	19.75	10.47
^{234}Th	19.3	15*	19.35	-	-	-	18.8	12.45

* Suspended sediments from the pump (average sample of 1 month)

Table S-3. Measured values of log Rd of the stable elements (L/kg). *literature search taken from J.D. Allison and T.L. Allison, 2005, SPM/Waterlog Kd, L/kg **literature search taken from Sheppard et al., 2009

	COP-1	COP-2	COP-3.1	COP-3.2	COP-3.3	COP-3 average	COP-4	COP-5	Average this	Median

									study	literature*
K	3.71	3.62	3.67	3.72	3.62	3.67	3.69	3.64	3.67±0.04	-
Cs	6.00	6.06	6.01	6.36	6.27	6.14	6.36	6.32	6.19±0.15	4.23**
Sr	3.10	2.95	3.06	3.07	3.02	3.04	3.06	3.12	3.05±0.05	2.68**
Ba	4.05	3.67	4.01	4.04	3.99	3.95	4.26	4.85	4.10±0.32	4.0 (2.9 -4.5)
Co	5.14	5.44	5.13	5.20	5.10	5.20	5.46	5.81	5.31±0.23	4.7 (3.2 – 6.3)
Ni	4.56	4.60	4.49	4.48	4.35	4.50	4.70	4.91	4.57±0.16	4.6 (3.5 – 5.7)
Cu	4.88	4.84	4.95	5.19	5.14	5.00	5.15	5.35	5.06±0.16	4.7 (3.1 – 6.1)
Zn	4.95	4.94	5.01	4.96	4.89	4.95	4.92	4.95	4.95±0.03	5.1 (3.5 – 6.9)
Ag	-	-	5.50	-	-	5.50	5.50	-	5.50±0.00	4.9 (4.4 - 6.3)
Cd	5.17	4.74	5.04	5.40	5.29	5.13	5.17	5.26	5.15±0.19	4.7 (2.8 – 6.3)
Pb	6.11	5.88	6.03	6.17	6.11	6.06	6.07	6.14	6.07±0.08	5.6 (3.4 – 6.5)

Table S-4. Measured values of log Rd of the radionuclides (L/kg).

	COP-1	COP-3	COP-4	COP-5	Average this study
^{40}K	3.73	3.72	3.72	3.28	3.61±0.22
^{137}Cs	≥5.37	≥ 4.62	≥5.26	≥5.00	≥5.06±0.33
^{7}Be	4.35	4.46	4.36	3.84	4.25±0.28
^{60}Co	≥4.02	≥4.02	≥4.35	≥3.82	≥4.05±0.22

^{210}Pb	4.09	4.94	4.91	≥4.44	4.64±0.48
^{234}Th	3.76	3.75	3.65	3.54	3.68±0.10

Table S-5. Modelled values of log Kd (L/kg).

	COP-1	COP-2	COP-3	COP-4	COP-5
Cs	4.53	4.35	4.50	4.48	4.51
Be	4.68	-	4.56	4.63	4.54
Sr	2.63	2.30	2.30	2.21	2.30
Ba	2.33	2.24	2.41	2.22	2.33
Co	4.13	4.43	4.18	4.28	4.42
Ni	4.25	4.30	4.22	4.23	4.30
Cu	5.03	4.94	5.12	5.11	5.18
Zn	4.75	4.73	4.71	4.64	4.74
Ag	2.00	2.68	2.05	2.15	2.01
Cd	5.13	4.88	5.20	5.10	5.17
Pb	6.00	5.86	5.99	5.98	6.00
Th	4.99	-	5.14	4.91	4.97

Table S-6. Prediction of NICA-Donnan parameters for the metal binding by fulvic and humic acids from the first hydrolysis constant (K_{OH}) by Milne (2001, 2003).

$n_1 = 0.13 - 0.056 \log K_{OH}$

$n_2 = 0.77 n_1$

$n_1 \log K_1 \text{ (fulvic)} = 0.36 \log K_{OH} + 2.47$

$n_2 \log K_2 \text{ (fulvic)} = 0.91 \log K_{OH} + 9.02$

$n_1 \log K_1 \text{ (humic)} = 0.26 \log K_{OH} + 2.55$

$n_2 \log K_2 \text{ (humic)} = 0.40 \log K_{OH} + 4.93$

	Ag	Cs	Th
$\log K_{OH}$	-11.997 -15.6847	-3.197	
n_1	0.80	1.01	0.31
n_2	0.62	0.78	0.24
$\log K_1$ (fulvic)	-2.306	-3.150	1.65
$\log K_2$ (fulvic)	-3.073	-6.766	25.46
$\log K_1$ (humic)	-0.710	-1.515	5.44
$\log K_2$ (humic)	0.213	-1.731	15.21